

Article

Optimising Daylight and Ventilation Performance: A Building Envelope Design Methodology

Rana Abdollahi Rizi ^{1,*}, Hamed Sangin ², Kiana Haghighatnejad Chobari ², Ahmad Eltaweel ³
and Robyn Phipps ¹ 

¹ Wellington School of Architecture, Victoria University of Wellington, Wellington 6011, New Zealand

² Department of Environment, Land and Infrastructure Engineering (DIATI), Politecnico di Torino, 10129 Turin, Italy; hamed.sangin@studenti.polito.it (H.S.); kiana.haghighatnejadchobari@studenti.polito.it (K.H.C.)

³ School of Computing, Engineering and the Built Environment, Edinburgh Napier University, Edinburgh EH10 5DT, UK

* Correspondence: rana.abdollahiriz@vuw.ac.nz

Abstract: The future of building envelope design lies in smart adaptation. The current literature overlooks the crucial integration of airflow, ventilation and daylighting in adaptive façade design. Moreover, it neglects the occupants' locations, activities and interior layouts in this context. This study introduces an innovative approach to adaptive building envelope design, aiming to enhance occupants' comfort through parametric analysis of daylight and airflow. The research combines parametric simulation, computational fluid dynamics (CFD) analysis and multiobjective optimisation. The optimisation goal is to improve visual comfort and indoor air quality while maintaining air temperature and velocity within the human comfort range. The study contributes to providing designers with a method for building envelope design that considers visual comfort and airflow, resulting in more interactive building envelopes that are adaptable to environmental conditions for enhanced utility and comfort. Results indicated that the optimised façade configuration and design methodology can achieve a 69% improvement in daylight performance, improving useful daylight illuminance (UDI) while reducing glare risk. Additionally, air changes per hour (ACH) showed a 38% annual improvement. This research signifies a significant step towards more efficient and occupant-centric building envelope design, aligning with the evolving demands of the construction industry and sustainable building practices.

Keywords: adaptive façade design; airflow; daylight; optimisation



Citation: Abdollahi Rizi, R.; Sangin, H.; Haghighatnejad Chobari, K.; Eltaweel, A.; Phipps, R. Optimising Daylight and Ventilation Performance: A Building Envelope Design Methodology. *Buildings* **2023**, *13*, 2840. <https://doi.org/10.3390/buildings13112840>

Academic Editor: Antonio Caggiano

Received: 5 August 2023

Revised: 27 October 2023

Accepted: 7 November 2023

Published: 13 November 2023



Copyright: © 2023 by the authors. Licensee MDPI, Basel, Switzerland. This article is an open access article distributed under the terms and conditions of the Creative Commons Attribution (CC BY) license (<https://creativecommons.org/licenses/by/4.0/>).

1. Introduction

Building envelopes serve as interfaces between indoor and outdoor environments and are significant components in improving human comfort and building energy efficiency [1]. As a critical success factor for a sustainable building environment, adaptation aids in coping with variable environmental conditions (e.g., solar radiation and wind) instead of anticipating potential damages and uncomfortable conditions for humans [2]. Kinetic architecture has been an adaptation technique since 1970 [3] and the parametric approach as a design method has helped eliminate many uncertainties associated with static and traditional methods of architectural design [4]. Parametric design tools aid in providing multiple solutions to geometrical problems while allowing for updates to input and output design parameters at any stage of the design process [5,6].

Incorporating morphological design parameters into optimisation processes is necessary for achieving optimum architectural solutions. The morphological aspects of building envelope design can significantly impact occupant comfort and satisfaction, and environmental simulation serves as the basis for initiating the formulation and design of adaptive

façades. This is because it empowers designers to evaluate how diverse façade configurations respond to fluctuating environmental conditions and their direct impact on human comfort [7,8]. Therefore, to adapt to the dynamic fluctuations of external environmental conditions, it is suggested that a combination of form-finding approaches, parametric methods and optimisation processes be used to respond to various weather conditions [9].

This study introduces a parametric methodology that optimises building envelope performance, prioritises visual comfort and airflow and enhances utility and occupant well-being, with a primary focus on beauty salons. These dynamic environments pose challenges due to extended client stays and chemical use, necessitating effective ventilation. Additionally, staff require glare-free illumination for sensitive tasks on their work plans. This research addresses a critical gap in building envelope design by emphasising the integration of airflow, ventilation, daylighting and occupant considerations. Neglecting these factors can compromise comfort and energy efficiency, necessitating a comprehensive approach. While daylight and ventilation are often studied separately, integrating both with attention to space utility, spatial layout and human activity is often overlooked. Additionally, when daylight and ventilation are studied separately, the improvement of one could potentially result in the worsening of the other.

The study hypothesises that by integrating parametric daylight simulation, CFD analysis and linear multiobjective optimisation, and taking into consideration interior spatial layout, occupants' locations and their activities, adaptive building envelopes can be created to significantly enhance indoor environmental quality. Specifically, the goal is to develop a methodology to enhance visual comfort and air quality while maintaining a comfortable range of air temperature and velocity for human comfort, thereby contributing to sustainable and occupant-centric building design practices.

2. Literature Review

Adaptive façades have emerged as a critical component of building design, with a particular emphasis on enhancing visual comfort. In recent years, remarkable progress has been witnessed in the areas of form-finding, morphological optimisation and automatic control of adaptive façades, mostly aimed at enhancing visual comfort in buildings. The process of form-finding in adaptive façades has undergone a transformative shift, with architects and engineers increasingly turning to parametric modelling and generative algorithms to create innovative façade designs.

These methods enable the optimisation of façade morphologies to manage natural light penetration and minimise glare [9]. For instance, Eltaweel and Su [10] showcased the use of parametric modelling to design a responsive façade that dynamically adjusts its shape to optimise daylighting and visual comfort throughout the day. A set of louvers responded parametrically to the sun's movement, aiming to manage the daylight inside the building envelope to achieve visual comfort for the occupants. These louvers parametrically reflected part of the sun's rays over the ceiling surface, allowing effective daylight distribution in south-oriented façades located in the Northern Hemisphere. Eltaweel and Su [1] explored various scenarios for louver configuration, striving to identify the most effective combinations. In a related study, Fahmy et al. [11] presented a kinetic façade system designed to enhance daylighting performance in buildings with western orientations by dynamically responding to the sun's position. Additionally, an integrated parametric simulation-based approach has been developed to optimise roller shade control. This approach aims to balance various occupant comfort factors, including daylight, glare, outdoor views and thermal comfort, while also managing HVAC efficiency [12].

In addition, there are also approaches that explored complex parametric geometries for adaptive façades to improve visual comfort [13]. In comparison to the performance of conventional static shading in the same location and test cell, the point-in-time evaluation indices for visual comfort quantity showed better daylight performance with the proposed kinetic south-oriented façade [14].

Researchers often employ a combination of parametric and simulation methodologies to investigate the morphological aspect of adaptive façades and assess their impact on improved visual comfort performance. This approach incorporates both annual indices, such as the useful daylight illuminance (UDI), and point-in-time indices, including glare indices and illuminance measurements. This multifaceted evaluation approach allows for a comprehensive analysis of visual comfort, considering both long-term performance trends and momentary conditions [15].

Integrating the user/occupant and their comfort needs into façade design constitutes a pivotal enhancement in the creation of adaptive façades. This approach signifies a commitment to elevating the quality and functionality of architectural solutions. It enables designers to craft façades that align with occupants' comfort needs [16]. This consideration not only fosters a heightened sense of well-being but also enhances overall building performance. Traces of this user-centred architectural design approach can be found in traditional architectural practices around the world. In vernacular architecture, buildings have long been shaped by the needs and comfort of their inhabitants. In modern practices, however, such importance is often neglected [17].

For integrating users into adaptive façade design for improved natural ventilation, there is a lack of methodology in the parametric style of design and practices. By integrating aspects of occupants' behaviour with other environmental stimuli and engineering considerations, the adaptive building envelope can achieve a higher level of functionality.

Building on the idea of integrating occupants and their needs into adaptive façade design, recent studies have explored innovative approaches. In a study by R. A. Rizi and A. Eltaweel [18], a parametric adaptive façade design method was proposed, which utilised innovative geometry to address occupant task surfaces and locations in order to enhance their comfort. Additionally, in the pursuit of improved visual comfort through a transformable façade, Hosseini et al. [19] parametrically incorporated the occupants' locations within the space, aiming for an interactive and robust façade design. The design utilised modular geometry capable of transformation in depth and opening areas.

Expanding on the notion of integrating users into adaptive façade design, especially when it comes to enhancing natural ventilation while considering visual comfort, it is important to note that there is currently a lack of methodology in parametric design and practices [20].

Natural ventilation offers significant potential for cooling and enhancing indoor air quality (IAQ) within non-air-conditioned buildings, especially in dry, mild and temperate climate zones. This potential can be used to design adaptive building envelopes that not only make the indoor environment more comfortable but also improve the health and well-being of the people inside [21,22].

In the process of natural ventilation, airflow forces and buoyancy help to provide the space with outside fresh air via airflow distribution. The factors influencing the efficacy of natural ventilation control encompass several key elements, including façade design, window dimensions, window shape, their placement on façades, the type of openings they provide and their respective areas and angles. Additionally, the impact of shading geometry is significant. Furthermore, dynamic environmental conditions and the arrangement of furniture within the space can influence natural ventilation control, some of which are neglected during the initial design phases [23]. For effective natural ventilation and guided airflow, architectural design aspects including form, context, spatial layout, human location and surrounding environment should be considered as influencing factors [24,25].

Yoon and Malkawi [26] employed a parametric approach to evaluate natural ventilation in various design alternatives, providing insights into the energy performance of building envelope solutions. Building on this, a subsequent study [27] utilised parametric methods to investigate wind-induced airflow in a façade design conducive to cross ventilation. This was achieved through CFD simulations and optimisation techniques, assessing curved façade morphologies to identify optimal airflow velocities for enhanced occupant comfort.

In another research study [22], the efficiency of cross-ventilation and single-side ventilation using ventilation panels was assessed for a high-rise building unit. Airflow velocity and air changes per hour (ACH) were calculated, demonstrating a fourfold improvement in airflow velocity and a 27% increase in ACH with the use of ventilation panels compared to conventional building configurations. These improvements were contingent on external wind speed and building location.

Furthermore, Arinami et al. [28] evaluated the impact of opening guide vanes and adjacent structures on the quality of single-side natural ventilation. They employed a methodology involving computational domains and fluid dynamic simulations, which revealed enhanced airflow within guide vane surfaces. As a potential avenue for future research, they highlighted the importance of optimising the location, size and angles of openings and guide vane surfaces, particularly in the context of cross ventilation.

In their study, Assimakopoulos et al. [29] calculated airflow rates for various window sizes and opening configurations to regulate natural ventilation. Similarly, Sacht and Lukiantchuki [30] evaluated and compared how different window sizes influence the natural ventilation conditions using CFD simulations. Their research did not take into account the use of window shading, however. There are also instances of articles that have concentrated on foldable adaptive shading systems intended for wind generators but they do not incorporate the redirection of airflow for interior ventilation coupled with enhanced visual comfort [31].

Integrating daylight and ventilation within a multiobjective façade design yields several objective advantages compared to evaluating each aspect separately. By strategically combining considerations for both daylight and ventilation, designers can harness the dual advantage of redirecting airflows for improved natural ventilation, effectively creating shadings that are multifunctional, adaptable and occupant-centric. In this way, the integration harmonises crucial environmental, economic and human factors, delivering a comprehensive and efficient solution [32–34].

Passive and active façade design strategies are fundamental tools, as well as a design approach, especially for commercial projects. By integrating sunlight, airflow and temperature data from climate sources during the initial design phases, a new architectural sensibility can emerge, with a focus on optimising daylighting and ventilation performance [35]. For instance, the prototype in K. Johnsen, et al.'s article [36] serves as an example of a smart façade incorporating exterior modules capable of vertical and horizontal movement to enhance solar heat gain, ventilation and daylighting. The system's geometry has been intentionally kept simple due to limitations in available marketable frames and materials. It has also undergone experimental testing to validate its proof of concept. Therefore, unconventional parametric geometry potential has not been explored in the system's morphology.

The Albahr towers feature one of the earliest examples of a complex parametric façade morphology designed to serve as both shading and wind protection [37]. The innovative skin of the towers was carefully crafted and implemented to provide these functional benefits while enhancing the buildings' aesthetic appeal. To protect against undesirable environmental effects, the Albahr towers' façade is designed to dynamically respond to environmental fluctuations. The façade features openings that can be closed or adjusted as needed to provide the necessary level of wind and sand protection from the exterior part of the windows. This enables the buildings to maintain a comfortable and safe interior environment even in challenging weather conditions. Additionally, the mechanism for ensuring interior visual comfort involves shading the space from incident solar radiation. However, the mechanism is kept simple for open and closed scenarios in response to occupants' activities and task locations. Therefore, no intermediate or calculated scaled opening fixtures are included for directed ACH [37].

Expanding upon the concept of integrating sun shading and airflow, Sun et al. (2018) [38] evaluated a laboratory building's façade by calculating airflow, wind velocity and daylight uniformity. The results indicated that the sunshades improved the thermal conditions

and reduced energy consumption of the building when compared to limited scenarios of shadings that used daylight simulation and CFD analysis without detailed consideration of the physical layout.

Omar Elshiwihy and Nasarullah Chaudhry [39] conducted a parametric study on external and internal shading devices and established their impact on energy consumption, daylight levels and ventilation. The work involved simulation CFD and numerical methods. The results revealed that optimised shading can positively influence the enhancement of daylighting, reduction of glare and improvement in ventilation parameters. Despite all external and internal shading options showing improvements, the egg crate shade was determined to provide the optimum energy savings while enhancing daylight and improving natural ventilation for sustainable building design. Egg crate shades are a type of light diffuser used to control and soften the brightness of overhead lighting in buildings. They resemble a grid or lattice of small, interlocking cells, similar to the shape of an egg crate. Traditional practices have commonly included this approach [40]. However, the use of unconventional geometries in a parametric context has only recently begun to be applied for parametric daylight management [41], and it has not yet been widely used for ventilation management.

3. Materials and Methods

The methodology employed a parametric approach, utilising the Grasshopper plugin of Rhino to define design inputs and parameters. Grasshopper excels in generating unconventional forms, managing design variables and integrating environmental analysis plugins within its graphical environment [42,43]. Through this parametric approach, the methodology investigated evaluation criteria and an optimisation process to enhance visual comfort, ventilation and airflow, taking into account occupants' locations and interior spatial adjustments. The method followed a parametric approach to propose and assess an adaptive façade design, comprising four crucial steps. These steps relied on specialised software tools, metrics and criteria to address key aspects.

In the first step, modelling, the focus lay on building a foundation for the subsequent phases. It encompassed the modelling of the conventional, current scenario, allowing for a baseline comparison against potential transformations. Furthermore, this stage involved setting crucial assumptions and identifying independent variables, which served as the building blocks with a transformable façade for the entire methodology.

The second step, environmental analysis, delved into the examination of climatic data. It involved the analysis of wind data extracted from weather files. Wind infiltration assessments were conducted based on wind speed, temperature and wind direction. The initial prerequisites for daylight analysis were established, including the preparation of essential elements such as the sky matrix, the daylight exposure environment, the interior 0.35×0.35 m grid for illuminance analysis on task surfaces and occupants' field of view settings [44]. Critical daylight availability settings were also configured. This step enabled a detailed understanding of the environmental conditions that will impact the design.

Step three, simulation, involved the in-depth examination of how the building's exterior and geometry influenced the indoor environment. This stage included critical components such as daylight simulation and the application of CFD techniques, accompanied by mesh independence analysis. These simulations helped in predicting how design choices affected occupant comfort and environmental performance.

The final step, optimisation, was the culmination of the entire process. It encompassed multiobjective optimisation, which harmonised the insights gained from previous steps. This step involved connecting the findings to the weather file and wind analysis, setting specific comfort criteria and selecting performance indices to guide the design. The establishment of boundary conditions ensured that the design aligned with the project's goals, followed by the implementation of criteria-driven ventilation strategies. The iterative nature of this step ensured that the design continuously evolved and improved, culminating in an optimised and environmentally responsive built environment.

Figure 1 illustrates the step-by-step methodology for integrated design and optimisation, showcasing the tools employed at each stage.

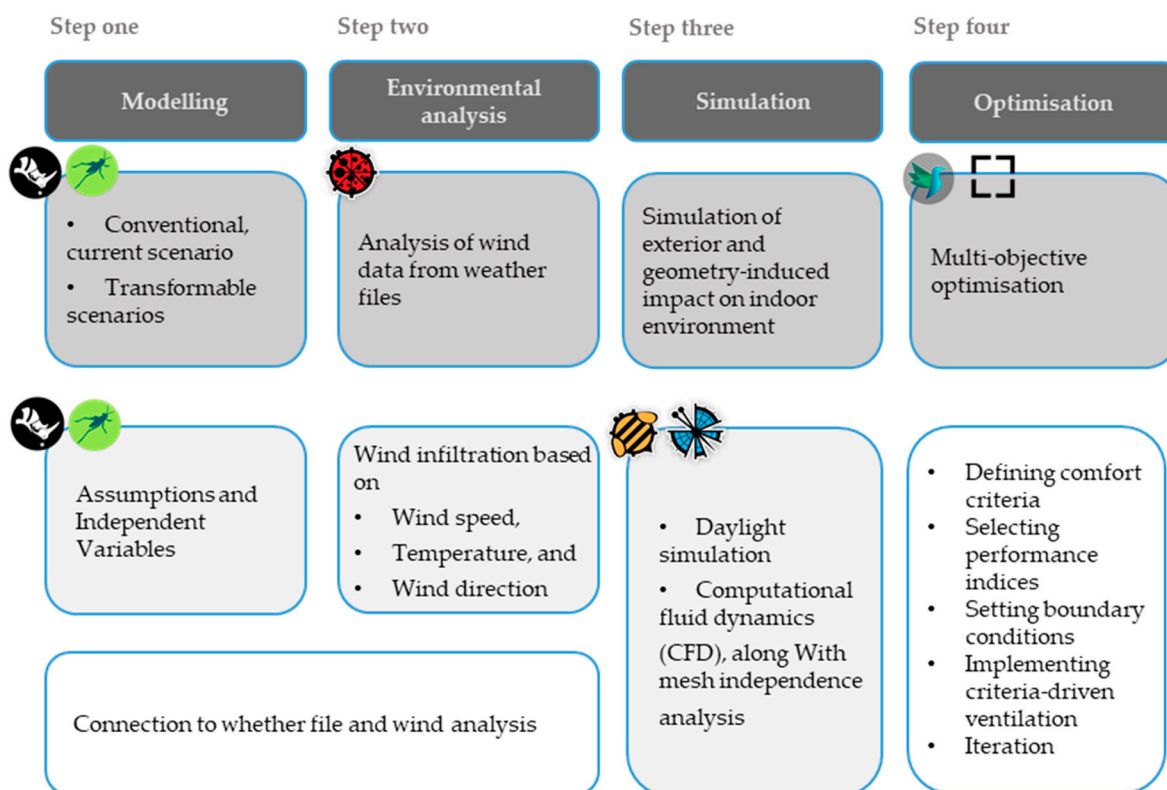


Figure 1. Integrated design and optimisation process: tools and methodology.

3.1. Case Study and Assumption

To conduct this research, a beauty salon located in Tehran, Iran, a region rich in daylight in the Northern Hemisphere [45,46] was used as a test cell.

Research on the indoor air quality of beauty salons has revealed that occupants' exposure to various cosmetic chemicals, typically used in these spaces, can substantially impact their health. This is especially concerning when it comes to the levels of volatile organic compounds in the space [47]. The activities performed in beauty salons require a high level of concentration, especially with regard to visual comfort. Excessive glare, whether from sunlight or reflections off furniture, can reduce people's productivity and their tolerance for uncomfortable conditions in these spaces. Therefore, a well-balanced natural ventilation system, in conjunction with the proposed façade in this study, would benefit the occupants while also potentially reducing energy consumption as a by-product of this process.

Figure 2 illustrates the current setup of the test cell, showcasing its layout, furniture, dimensions and the location and posture of the occupants. The salon can accommodate six employees, including four seated around the central task surface and two standing in front of mirrors. Both the task surface for seated occupants and that for standing occupants are depicted in Figure 2. For sitting occupants, the evaluation surface is located at a distance of 0.7 m above the floor. For standing occupants, a one-by-one hypothesised evaluation surface is allocated, with each one located 1.2 m above the floor, serving as a representation of the task surface. In the current space, there are two openings: one in the south-oriented façade and the other in the north façade. Both windows are vertically operable.

The test cell design draws inspiration from many female beauty salons in Tehran, where immediate outdoor access and street views are often limited. The central area is typically used for nail trimming and polishing, with wall mirrors in the surrounding space for chemical applications. To comply with health regulations, the salon owner must choose

a location approved by the authorities, including windows for natural ventilation. This spatial layout can be found in some other countries too [48].

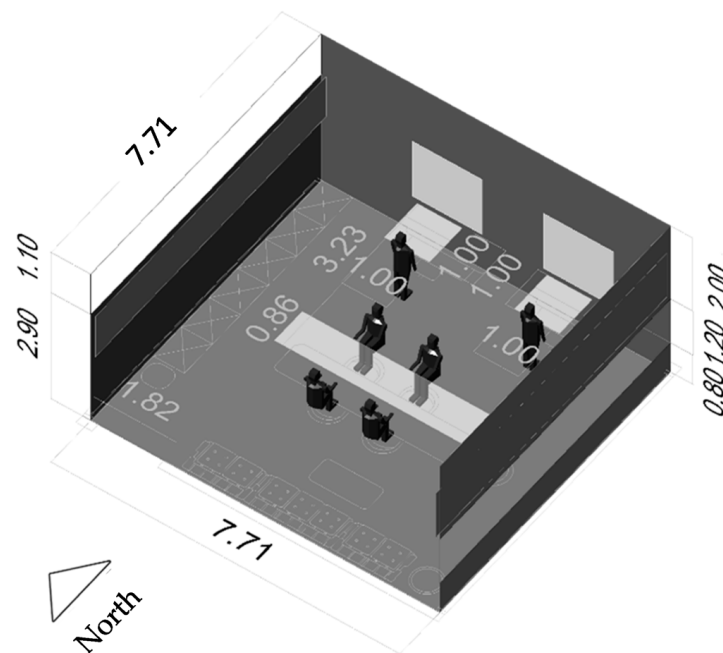


Figure 2. The test cell, spatial layout and dimensions.

Independent Variables

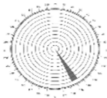
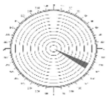
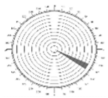

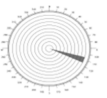

The south window of the test cell is 1.20 m high and the same length as the wall. This window is 0.8 m above the floor level while the north window is 1.10 m high and the same length as the wall. This window is 2.90 m above the floor level. The height of the south window was further set as one of the independent variables for the optimisation process while the dimension of the north window was kept the same as the current condition. Both windows are kept open during the simulation process.

After modelling the geometry of the space in the Autodesk Rhino 3D environment, critical daylight availability dates, year-round, in the region, were detected [10]. The minimum and maximum daylight availabilities, 21 December and 21 June, respectively, were the critical dates selected for the simulation and optimisation process in this paper. Furthermore, the morning, noon and afternoon times—10 a.m., 1 p.m., and 4 p.m., respectively—were chosen in accordance with the methodology outlined in references [10,14]. These selections were made to encompass the most probable daylight availability scenarios that occur in this region. Table 1 displays the critical times of the year in terms of daylight availability and the wind characteristics on those days, which were selected for natural ventilation in this study. Consequently, the dates for CFD analysis were restricted to align with those used for daylight analysis. This adjustment was made to narrow down the scenarios for conducting CFD analysis, given the resource-intensive nature of this analysis in terms of both time and hardware limitations.

Following this, an examination of the dominant wind directions and their potential for enhancing natural ventilation and improving ACH (air changes per hour) was conducted. This analysis was based on parameters such as airflow speed and air temperature at the specified times. For wind speed analyses, Grasshopper, Ladybug, was used to import the weather data file. As for air temperature analyses, the Universal Thermal Climate Index (UTCI) was chosen rather than using dry bulb temperature. This way, a real sense of external airflow quality became attainable, since UTCI takes into account dry temperature, relative humidity, solar radiation and air velocity to demonstrate an environmental temperature [49]. The range for this criterion was selected to be between 20.30 °C and 26.7 °C [50]. This range

aided in evaluating the suitability of outside air for natural ventilation. Consequently, this classification was then employed to shape the design of the proposed façade morphology.

Table 1. The critical times of year in terms of daylight availability and wind potential for natural ventilation (Red: no direct natural ventilation potential; unpleasant wind. Blue: suitable for direct natural ventilation; pleasant wind).

Option/Number		1	2	3	4	5	6
Date	Season	Summer	Summer	Summer	Autumn	Autumn	Autumn
	Month	June	June	June	September	September	September
	Day	21th	21th	21th	21th	21th	21th
	Hour	10:00	13:00	16:00	10:00	13:00	16:00
Wind Properties	Wind Direction (Degree)	150	120	120	160	105	190
	Wind Speed in 5.5 (m/s)	3.8	3.82	2.29	3	0.4	1.5
	Wind Temperature (°C)	35.3	37	39.3	26.8	28.1	30
	Wind Direction						
Weather Information	Universal Thermal Climate Index (°C)	33	35.1	38.2	23	26.2	27

The red colour in Table 1 indicates the period during which airflow does not have the potential for natural ventilation. In this study, such airflows are termed unpleasant wind, while the blue ones represent periods appropriate for natural ventilation. These winds were termed pleasant wind. The proposed façade design aimed to enhance both of these airflows, thereby improving ACH and the comfort of occupants, while also taking into consideration the improvement in visual comfort for the occupants. Additionally, during times when the outside air was extremely cold or hot, or when the wind speed was very high, the windows were closed and the façade was served to control indoor lighting.

The façade geometry logic used in this paper was similar to that in the study conducted by Hosseini et al. (2019) [19]. However, there is a distinction in this study's objective, which focuses on developing a façade design methodology that enhances both visual comfort and airflow rates. In reference [19], the author utilised façade geometry to primarily enhance visual comfort, specifically considering the occupants' positions in an office space in Tehran.

The formation of the façade geometry began with gridding the southern wall and allocating each grid to a façade module.

The variables used to create the transformable geometry for each of the façade modules include horizontal movement, vertical movement, depth, opening scale (Figure 3) and sun position in the sky based on critical months and hours. To make the façade geometry responsive to both unpleasant and pleasant winds, the control mechanism in Figure 3 was utilised. The line between the centre point and the base of the pyramid of façade geometry modules is perpendicular to the unpleasant wind, while the line between the centre point and the base of this pyramid is parallel to the pleasant wind direction (see Figure 4). This design ensures that the interior space receives more pleasant airflow while diverting unpleasant airflow away from the interior.

Figure 5 illustrates the façade geometric variables along with their associated codes to be entered into the optimisation process for discovering the optimum shape. The depth of shading varies based on the geometric attraction point of the sun's location in the sky, with this parameter ranging from 0.0 m to 0.6 m. The scaling aspect of this formation relies on the geometric attraction of the distance from the sun's location in the sky, leading to a

remapping into upper and lower ranges. The mention of “Upper limit” and “Lower limit” percentages indicates specific thresholds or limits for these geometric transformations. The mathematical explanation of the attraction point is in the study carried out by Guo (2018) [51].

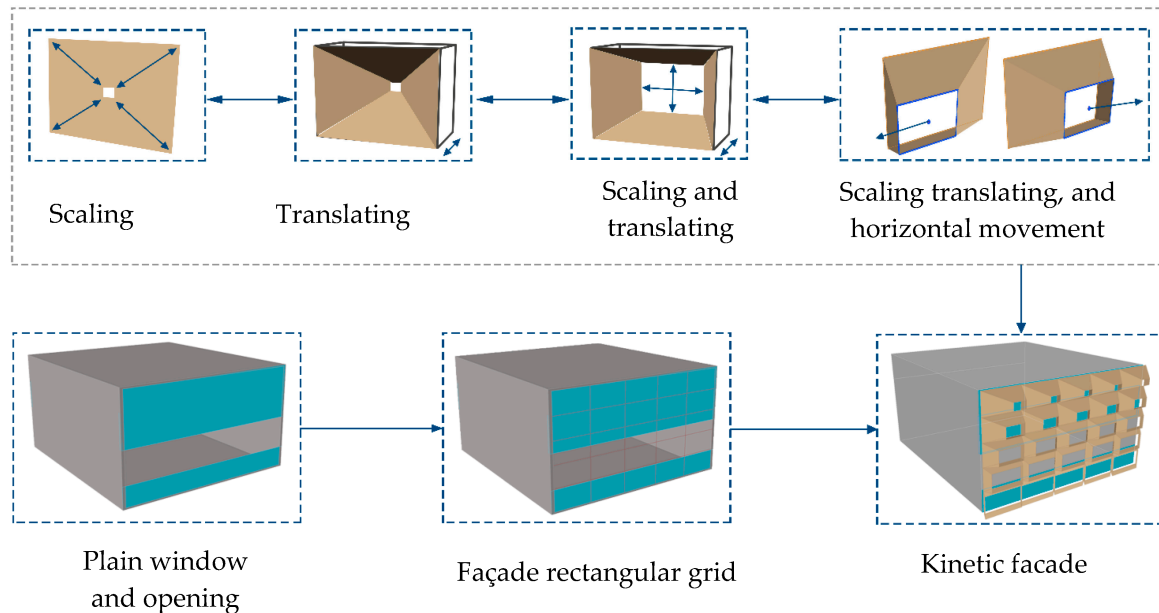


Figure 3. Parametric geometry formation of the kinetic façade: achieved through scaling, translation and their combination.

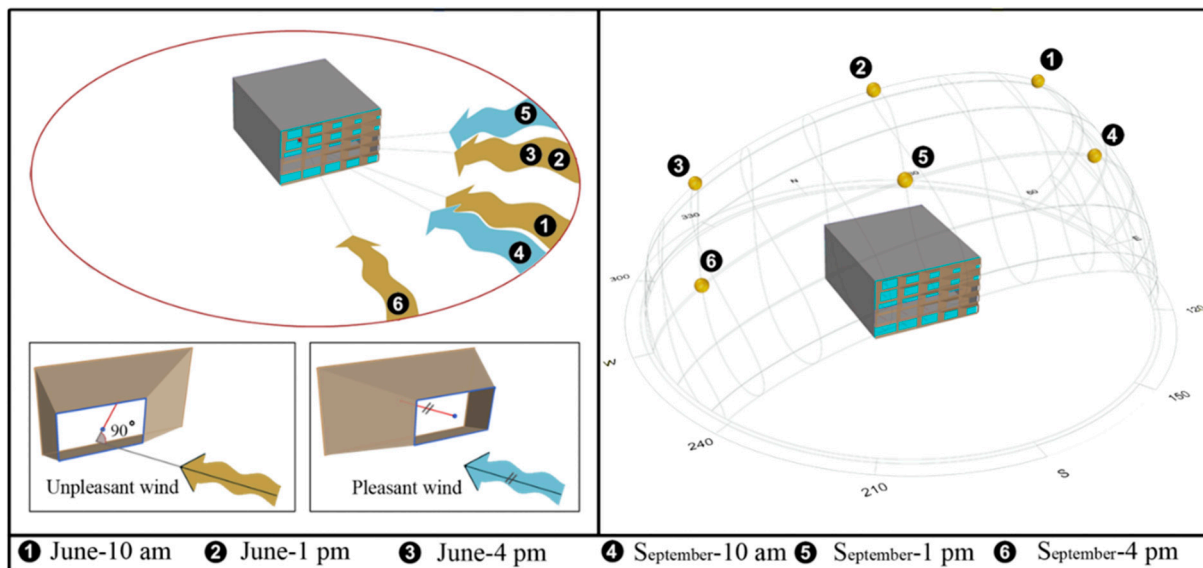


Figure 4. Effect of wind on the geometric inclination of panels (left), time of year of the effect of wind and daylight condition (right). The numbers in black circles are the time code to help illustrate time, sun’s position in the sky and wind direction.

For glare analysis, the locations of the occupants and their respective fields of vision were selected and named as P1, P2 and P3. These selections were made to encompass the most probable scenarios of occupants’ visual discomfort considering the furniture layout. Figure 6 illustrates these three locations and the directions of sight.

The material properties of the test cell and the proposed shading are outlined in Table 2. Furthermore, the selection of material reflectivity was determined through an initial test

conducted within a limited set of simulations to identify the reflective properties that would best enhance visual comfort results in various seasons.

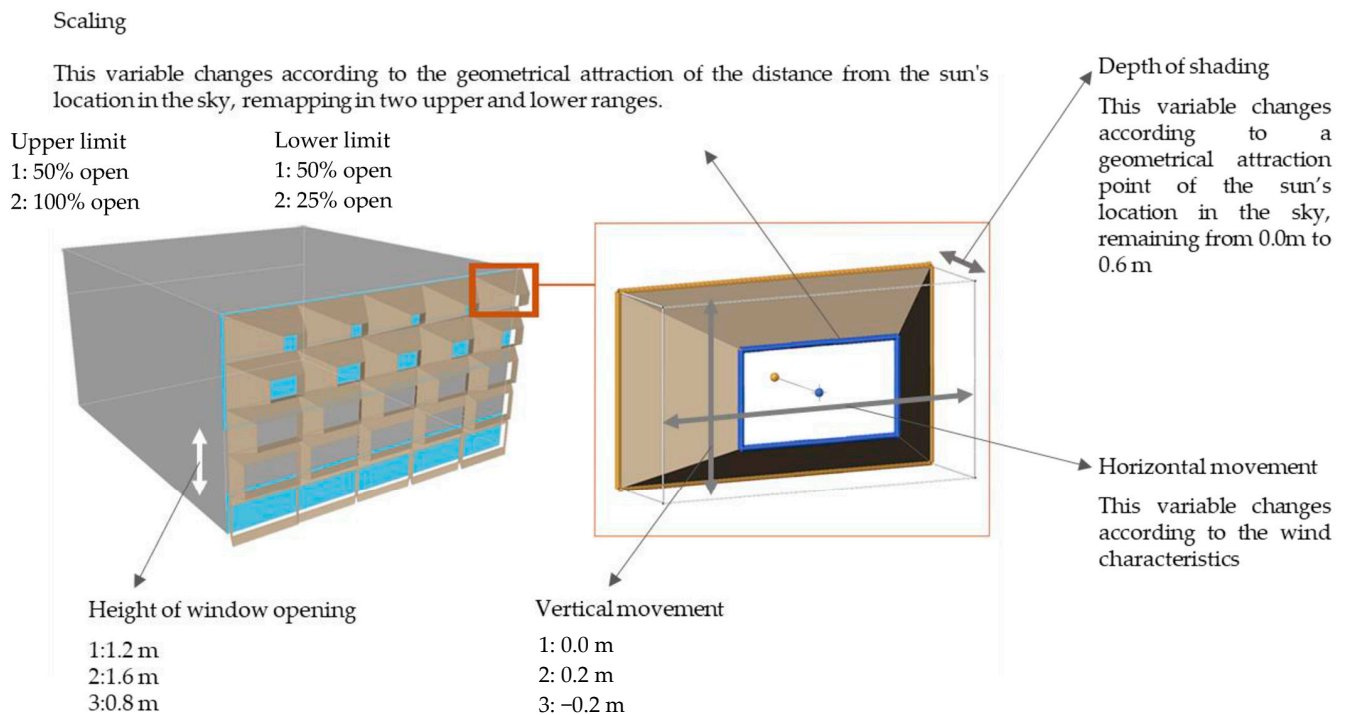


Figure 5. Façade geometry formation and variable attributes and codes to be entered into optimisation process for form finding.

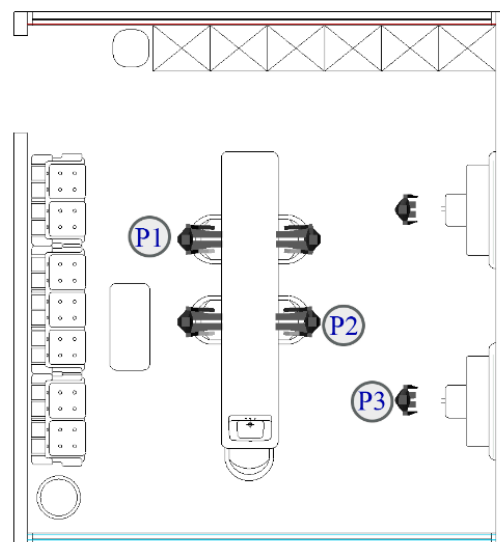


Figure 6. The three predefined occupants' location and view direction for the glare analysis.

Due to hygiene regulations, the need for easy cleaning, and the minimisation of chemical and dirt absorption, it is suggested that appropriate materials, such as ceramic, be used for the floors and walls in a beauty salon [52]. Ceramic tiles typically exhibit modest reflectivity towards solar energy, ranging from a maximum of roughly 60% down to a minimum of 17.3%. As a result, they can be considered effective at absorbing solar energy and are categorised as strong absorbers of solar radiation [53]. In this study, two different ceramics had been used for the walls and floor. The reflection property of the ground was learned from [54]. Additionally, the choice of material reflectivity was determined through an initial test conducted within a limited set of simulations to identify which reflective

properties would best suit visual comfort results in different seasons. Table 2 shows the material properties of the modelled elements. The materials were chosen from a range of white and beige tones because, in a hot climate, they exhibit lower thermal absorption properties [17].

Table 2. The material properties of the modelled test cell and its spatial layout and the proposed shading.

	Reflectance	Transmittance	Refraction Index	Roughness
Walls	50%	-	-	0.05
Ceiling	45%	-	-	0.05
Window glass	-	75%	1.52	-
Floor	30%	-	-	0.10
Ground	10%	-	-	0.05
Mirrors	99%	-	-	-
Desks	60%	0%	0	5%
The conventional shadings (concrete) [54]	30%	0%	0	5%
The proposed shading (textile) [54]	Reflectance: Red: 16% Green: 36% Blue: 2%	0%	Diffuse: 0.06% Specular: 0.1%	0.2%
Human body (Adopted from the article of Lister et al. [55])	7%	0%	0	25%

In this study, an optimisation process was used parametrically based on several variables of the façade morphology including height of openings, horizontal movement, vertical movement, depth and scaling (see Figure 3). These variables are introduced to the multiobjective optimisation environment to produce 216 alternative façade forms.

3.2. Visual Comfort Analysis

For assessing visual comfort, the Honeybee plugin was employed as a tool [56]. The Useful Daylight Illuminance (UDI) index was chosen for the annual daylight performance evaluation [57,58]. This index is defined as “the percentage of occupied time in a year when the daylight quantity in indoor environment falls in a predefined useful range”. This index includes a lower bound and a higher bound of the useful daylight ranges defined as Underlit UDI and Overlit UDI. The appropriate UDI falls within the range of 300 to 3000 lux (Table 3). The three above ranges defined for this study are presented in Table 3, following the range defined in the study by Nabil and Mardaljevic (2005, 2006) [57,58].

Table 3. Useful Daylight Illuminance ranges [59].

Useful Daylight Illuminance Ranges	
Underlit Useful Daylight Illuminance	Less than 300 lux
Appropriate Useful Daylight Illuminance	300–3000 lux
Overlit Useful Daylight Illuminance	More than 3000 lux

When greater luminance than what is versatile for the occupants’ eyes and visual activity exists in a space, visual inconvenience known as glare happens [44]. In this study, the Discomfort Glare Probability (DGP) Index was used to evaluate visual comfort quality. This index was defined by Wienold and Christoffersen (2005) [60] and validated by Wienold and Christoffersen (2005) [61]. For DGP analysis, the amount of illuminance

and the source of light, as well as the occupants' point of view, should be determined according to their position inside the space. For interpretation of the DGP results, the level of discomfort sensation is defined as more than 0.45 (intolerable), 0.35–0.40 (disturbing), 0.3–0.35 (perceptible) and less than 0.3 (imperceptible) [44].

To assess the glare based on the DGP Index, first, the amount of illuminance, the corresponding sources of light and the occupant's viewpoint were determined according to their position within the space. Then, a backwards render was performed using radiance in high dynamic range (HDR) format [62]. Consequently, Evalglare software (v1.04) was used to evaluate and detect glare in a 180-degree fisheye scenario [60]. The DGP formulation is shown in Equation (1).

$$\text{DGP} = 5.87 \times 10^{-5} E_v + 0.0918 \times \log_{10} \left[1 + \sum_{i=1}^n \left(\frac{L_{s,i}^2 \times \omega_{s,i}}{E_v^{1.87} \times P_i^2} \right) \right] + 0.16 \quad (1)$$

In Equation (1), E_v is the vertical eye illuminance produced by the light source (in lux). L_s is the source's luminance [cd/m^2] and the solid angle of the source viewed by an observer is ω_s . P stands for position index, which expresses the change in the perceived uncomfortable glare as a function of the source's angular displacement (azimuth and elevation) from the observer's line of sight.

3.3. Ventilation Analysis

Natural ventilation is a method to refresh the stagnant air inside a building with fresh outdoor air. This method relies on the inherent movement of air and does not rely on mechanical systems for operation. Instead, it harnesses passive physical processes like wind pressure and the stack effect. Natural ventilation openings can either be fixed or adjustable, with adjustable ones being either automatically controlled, occupant-operated or a combination of both. This approach is a vital element of environmentally friendly building design, contributing to improved indoor air quality, enhanced thermal comfort and increased energy efficiency. There are three primary types of natural ventilation that can be incorporated into building designs: single-sided, stack and cross ventilation [63].

Cross ventilation (which has been used in this study) is a type of natural ventilation that combines wind pressure and the stack effect to produce an airflow through a building. Cross ventilation necessitates openings on at least two sides of the building, and the wind pressure creates a pressure disparity that propels air through the building [63].

In a naturally ventilated building, the air is driven in and out because of pressure differences produced by wind and/or buoyancy forces. Three approaches are designated in the literature to study natural ventilation: empirical models, experimental measurements and CFD simulations. CFD simulation is becoming popular due to its informative results, low cost and requirement for little equipment [64]. In this study, CFD simulations were conducted using Ladybug Tools (Butterfly), where a set of simulation processes utilising validated engines was combined to create a hybrid workflow. The CFD simulations were conducted using the Butterfly tool [65] coupled with the OpenFOAM [66] interface to calculate ACH, velocity and temperature for natural ventilation.

The first step in setting up this simulation workflow was to create the geometric representation of the building's indoor and outer façade. For each geometry, the corresponding boundary conditions were also required. Consequently, boundary conditions for the surfaces of the geometries, including all building walls, roof, ground, floors and outer façade, were introduced into the algorithm.

Another step was to define a refinement level for the geometry. For the wall refinement, a boundary of (3, 3) was chosen. This refinement was used for snappy Hex Mesh to create high-quality hex-dominant meshes based on arbitrary geometry [67]. These refinements can flexibly improve the quality of the final mesh geometry, resulting in a higher resolution of edges, surfaces and inside or outside volume mesh geometry [68].

Butterfly has two types of indoor and outdoor airflow simulations. In this study, we incorporated an outdoor simulation scenario that included a surrounding volume to define the wind tunnel around the test cell. The inclusion of this surrounding volume serves several important purposes. Firstly, it ensures that the airflow in the simulation is fully developed both to the windward and leeward sides of the objects. This is crucial for accurately capturing the complex flow patterns around buildings and façades. Secondly, the surrounding volume allowed for the implementation of a refinement region, as suggested by Zhao et al. [69], where values were assigned to grid cells based on best practices for CFD modelling. Specifically, we applied up to three levels of refinement to all cells near the building and façade surfaces, following the recommendations in references [70–72].

To initiate the CFD analysis, the wind tunnel was configured to be four times the height of the building, extending five times further in front and to the sides and ten times downwind of the building to ensure undisturbed flow conditions [73]. Another critical step involved selecting the mesh type for the CFD simulations, as it directly influences the accuracy and efficiency of airflow modelling [74]. In our study, we initially employed structured meshes, which consist of grids composed of structured cells like hexahedra (in 3D) or quadrilaterals (in 2D) [75]. These meshes offer high orderliness and prove efficient for certain geometries, particularly those with well-defined boundaries. They were created using preprocessing tools such as snappyHexMesh and blockMesh in OpenFOAM, allowing for mesh generation and manipulation according to specific requirements [76].

In order to generate grid grading in the wind tunnel, a set of values, as listed in Table 4, was defined. These values determine the number and dimensions of cells for the CFD analysis mesh structure. The cell size value was the area of interest, which is illustrated in Figure 7 in red and the cell-to-cell ratio expansion ratio is how cells expanded. Also, the wake offset defines the length to be added to the end of geometry bounding box to be considered as part of the area of interest. Table 4 presents the tunnel grading settings.

Table 4. Assumptions for wind tunnel grading in the CFD simulation.

	Cell Size	Cell-To-Cell Size	Wake Offset	Height Offset
Value	1	1.2	2	5

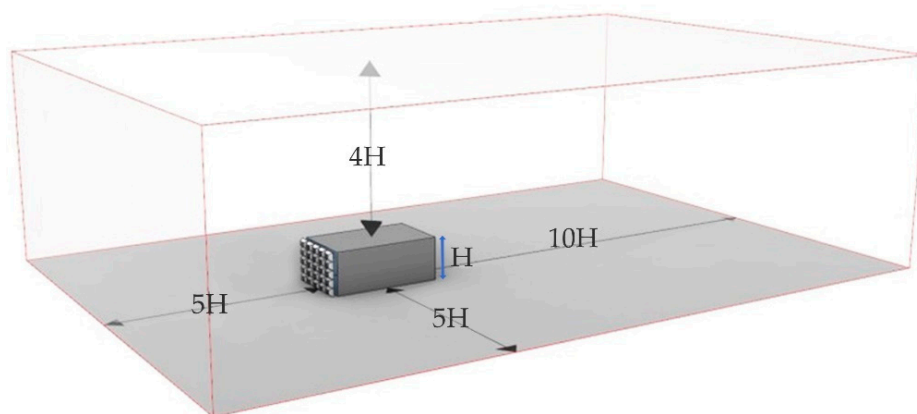


Figure 7. Refinement region around the test cell (“H” stands for building height).

The next step involved configuring the settings for snappyHexMesh to create high-quality hex-dominant meshes based on arbitrary geometry [67]. snappyHexMesh is a mesh generator tool that is part of the OpenFOAM software (V.5.x), specialising in generating three-dimensional unstructured or hybrid meshes [73]. In this study, the centre point of snappyHexMesh was positioned at the centre of the test cell and the refinement range for snappyHexMesh was set to (3, 3).

To create high-quality hex-dominant meshes that accurately capture intricate and arbitrary geometries, we meticulously applied a strategic refinement strategy with a boundary

of (3, 3) using snappyHexMesh tools. This strategy involves densifying the mesh near walls and areas of interest, significantly enhancing the fidelity of the mesh geometry. The increased resolution represented boundary layers, flow separations and other intricate flow phenomena, ensuring precise insights into fluid behaviour near surfaces during simulation. The finer mesh resolution ultimately leads to improved accuracy in analysing velocity, pressure gradients and other flow parameters [68].

A CFD analysis is divided into Reynolds-averaged Navier–Stokes equation (RANS) modelling and large eddy simulation (LES). RANS is a popular CFD method that uses turbulence models to simulate turbulent flow [64]. In this study, 3D steady Reynolds-averaged Navier–Stokes (RANS) CFD simulations were performed following previous studies and the amount of convergence was set to all the scaled residuals when they reached a minimum of 10^{-6} [77,78]. In other words, the CFD simulation process stopped when convergence reached within a certain tolerance. This tolerance was set to 10^{-6} for all variables.

Turbulence models, known as auxiliary equations, are essential in Reynolds-averaged simulations (RANS). Among the common RANS models, the K-epsilon ($k-\epsilon$) model has received the most attention to date. It is widely regarded as the standard model and serves as a primary reference for researchers in the field of urban aerodynamics [79,80]. In this study, the RANS turbulence model, specifically the K-epsilon type for incompressible RAS turbulence models, was selected to achieve the best possible results.

To carry out the process, the opening in the south façade was given to calculate ACH as an evaluating surface (see Figure 8). For this, test points were created to evaluate the velocity of air on this evaluated surface (U field prob). In addition, to calculate the velocity in outlet surface, temperature and pressure of airflow at occupants' task surface height (0.7-m) via CFD analysis in butterfly, the wall, floor and roof temperatures were calculated via EnergyPlus. The test cell dimension is further elaborated in Figure 2.

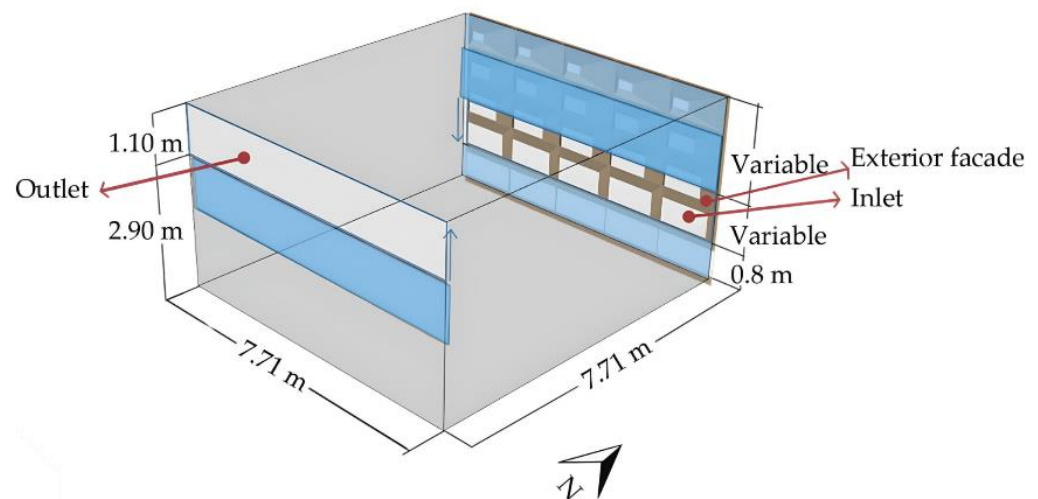


Figure 8. Test zone for CFD model in Grasshopper, displaying inlet and outlet surfaces, as well as building and façade surfaces (“N” represents north and “m” stands for metre).

3.3.1. Verifying Mesh and Grid-Sensitivity Analysis

In the pursuit of evaluating mesh-related errors' impact on CFD results, a grid independence analysis was conducted to ensure the reliability and accuracy of the outcomes. The primary goal of this analysis was to confirm that the choice of grid had a negligible effect on the results, and this process was streamlined and expedited through the use of an automated grid generation method [77,81].

To assess grid sensitivity, the velocity magnitude was meticulously assessed along a vertical line (positioned at the centre of the building at $x = 3.85$ m and $y = 3.85$ m, as depicted in the coordinate system of Figure 3). Moreover, the study included a comparative

evaluation of airflow rates across three distinct grids. To comprehensively assess grid sensitivity, three distinct grids were generated: a basic grid consisting of 44,880 cells, a coarse grid with 18,096 cells and a coarser grid with 13,680 cells. These grids were thoughtfully selected to provide a comprehensive insight into airflow velocity fluctuations within the central region of the room. This approach facilitates a detailed examination of how different grid configurations impact the accuracy and reliability of the airflow data, ensuring that the results are robust and can be trusted for further analysis and decision-making [82,83]. Figure 9 illustrates the location of the line used for assessing grid independence. The line is exactly located in the centre of the test cell.

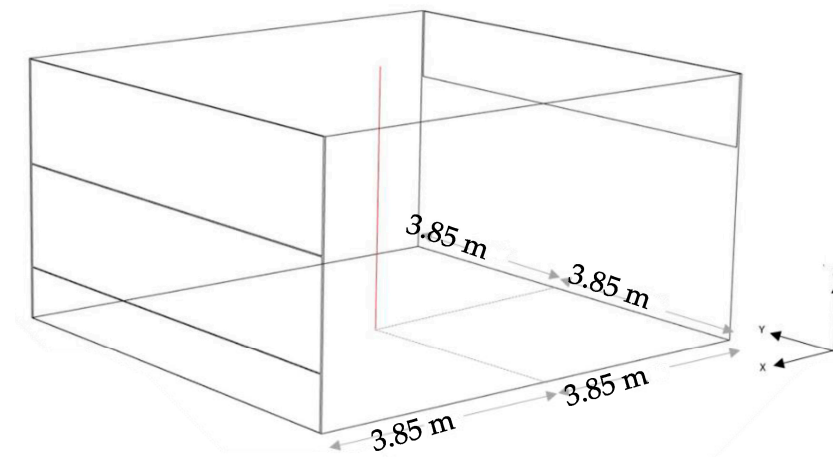


Figure 9. Position of the vertical line in middle of the room for grid-sensitivity analysis. m stands for metre.

Figure 10 illustrates the airspeed along a line positioned in the middle of the case study room. Comparative analysis of the results from the basic grid against the coarse grid and the coarse grid against the coarser grid showed average absolute deviations of 1.6% and 1.9%, respectively. These findings, in conjunction with considerations for computational efficiency, led to the selection of the basic grid for all subsequent simulations. This rigorous grid independence analysis establishes confidence in the reliability and accuracy of the CFD results.

3.3.2. Air Change per Hour

To analyse the airflow of the test cell, ACH was used. This means air changes per hour, abbreviated as ACH. In other words, the air change rate is a measure of the volume of air added to or removed from a space in one hour, divided by the volume of space [84]. The average of the inlet air velocity values, multiplied by the area of the outlet surface (as illustrated in Figure 8), indicates the discharge of airflow. Refer to Equation (2).

$$\text{Average Velocity (m/s)} \times \text{Area (m}^2\text{)} = \text{Air Discharge (m}^3\text{/s)} \quad (2)$$

Additionally, to calculate the air change rate in the room, the discharged air calculated from Equation (2) was divided by the volume of the test cell. Equation (3) shows the calculation process of the air change rate.

$$\text{Discharge (m}^3\text{/s)} / \text{Volume (m}^3\text{)} = \text{Air Change rate} \quad (3)$$

Finally, to calculate the amount of air change per hour, the air change rate was multiplied by 3600 (number of seconds in one hour). Refer to Equation (4).

$$\text{Air Change rate} \times 3600 = \text{ACH} \quad (4)$$

The calculations of Equations (1)–(4) all were carried out in Grasshopper software (V. 6).

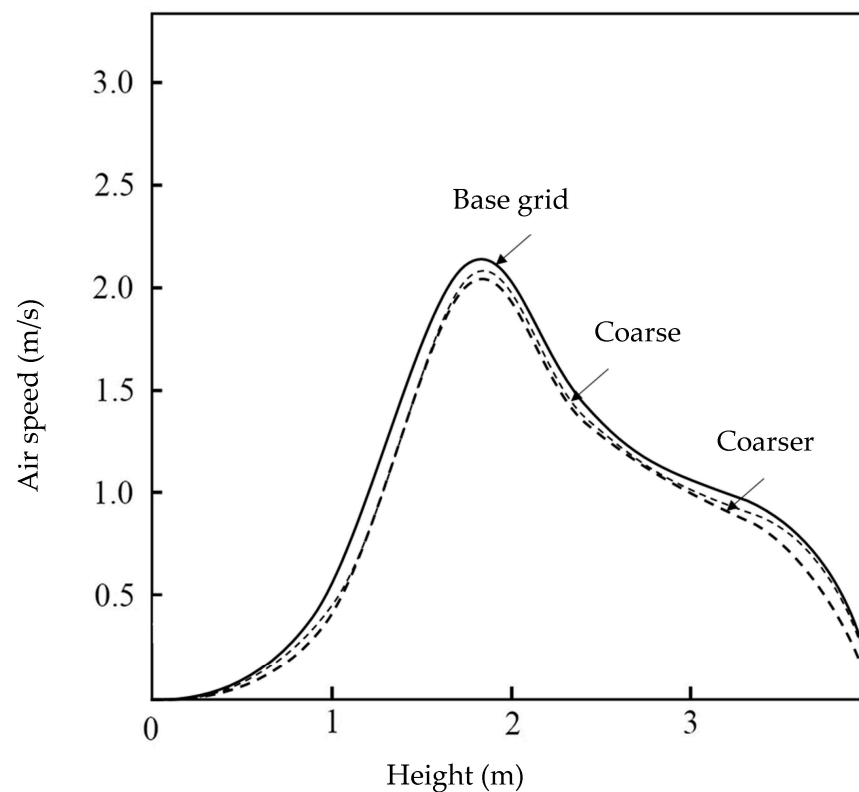


Figure 10. Visualisation of air velocity within the room along a vertical line positioned at the centre of the salon; m stands for metre, s stands for second.

3.3.3. Velocity, Temperature and Pressure

The properties of indoor airflow, including temperature, velocity and pressure, were calculated at a height of 0.7 m from the floor. Mobilised with the OpenFOAM engine, Butterfly allowed for incompressible flow and heat transfer calculations [85]. Additionally, the heat transfer output, which was associated with the temperature of the wind and the temperature of the walls, was extracted from EnergyPlus to calculate the interior air temperature and velocity at a height of 0.7 m from the floor.

3.4. Optimisation

For the optimisation, two objectives were defined: visual comfort and airflow improvement management by increasing ACH within the bounds of human thermal comfort. Under the category of visual comfort, the objective was defined as “increasing appropriate UDI while decreasing under-lit and over-lit UDI”. In addition, minimising glare was put forward. On the other hand, for airflow modification, the goal was to create an airflow between 0.1 and 1 m/s while maintaining an air temperature between 22.20 °C and 35 °C. To maintain occupants’ comfort, the goal was to minimise airflow when the temperature dropped below 22.20 °C and to reduce airflow when the temperature exceeded 37 °C. These conditions were defined to ensure that increased ACH would not negatively impact the occupants’ comfort. These thresholds were reported by ANSI/ASHRAE Standard 55 (2017) [50] and N. Lechner (2015) [19,86] as the trigger for occupants’ reactions to thermal dissatisfaction. Figure 11 presents the mechanism for multiobjective optimisation workflow.

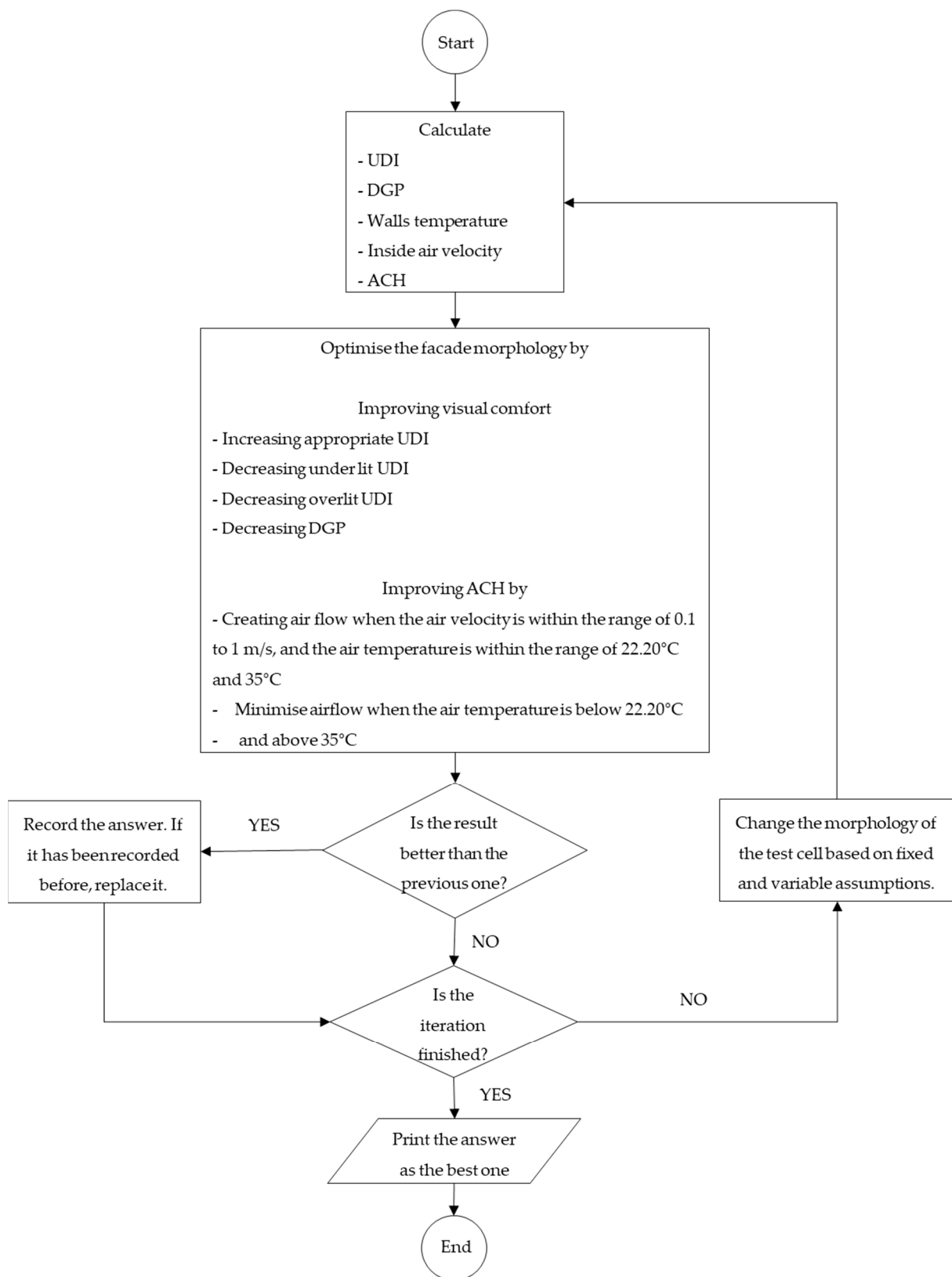


Figure 11. The multiobjective linear optimisation mechanism; UDI stands for Useful Daylight Illuminance, DGP stands for Discomfort Glare Probability and ACH stands for air change rate per hour.

4. Results

A concise summary is provided here of the noteworthy discoveries regarding occupants' comfort within the test cell. These insights encompass aspects of daylight and airflow performance, acquired through a simulation and optimisation process.

In the conventional test cell mode, the appropriate annual daylight performance, referred to as the “UDI appropriate”, was 27.97%. Notably, the overlit UDI was as high as 71.97%, with no instances of underlit UDI. This indicates an excessive influx of disruptive daylight, particularly in the context of a hot, arid climate. Such brightness can potentially result in visual discomfort and overheating issues. The simulation recorded instances of both disturbing and hardly perceptible glare caused by the conventional geometry of the test cell and shading in various occupant locations. To compare the conventional and optimal annual modes with the optimal façade of the test cell, Figure 12a,b display the corresponding colour maps of the appropriate UDI on the evaluation surfaces (occupants' task surfaces) for both modes.

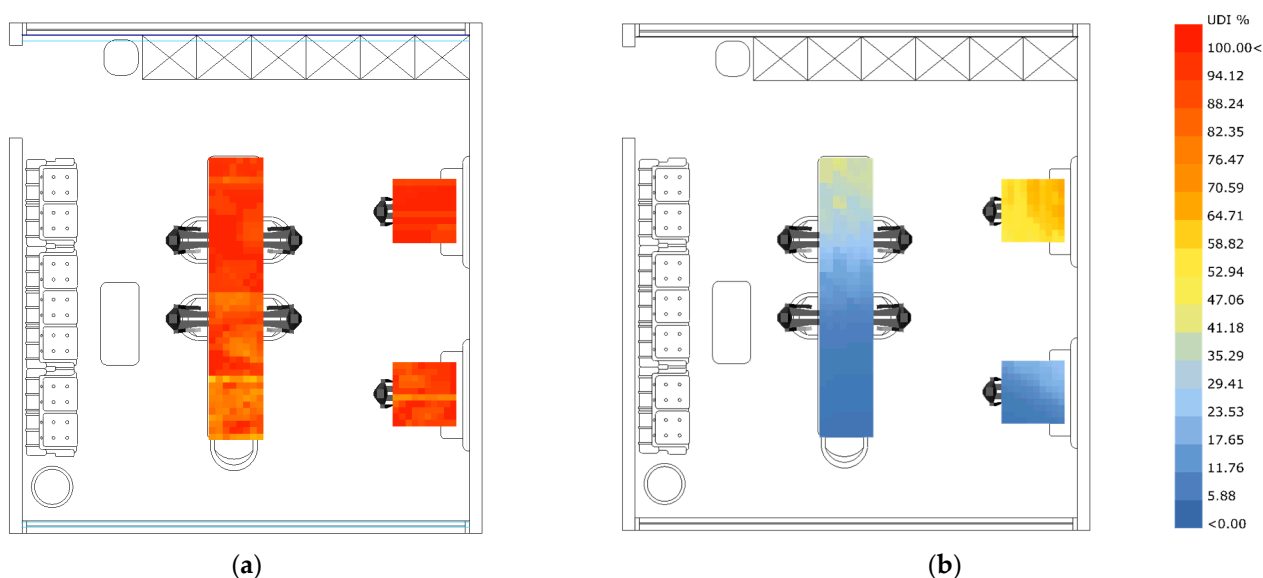


Figure 12. Annual daylight performance map (UDI appropriate): (a) optimal annual mode; (b) conventional mode.

The optimal annual mode (Figure 12a) reveals the improvements and optimisations implemented to enhance the distribution of daylight within the test cell. The conventional status (Figure 12b) provides a baseline reference point for evaluating daylight distribution throughout the year. These maps, when viewed side by side, offer a visual representation of the impact of optimisation strategies on the availability and quality of natural daylight. Additionally, Table 5 presents the glare analysis results, denoted as DGP, for the test cell, concerning three predefined occupants' positions (P1, P2 and P3).

Table 5. Glare analysis (DGP values) for the conventional mode, using a colour code where red represents intolerable glare, yellow indicates perceptible glare and green signifies imperceptible glare.

	June			September		
	10 a.m.	1 p.m.	4 p.m.	10 a.m.	1 p.m.	4 p.m.
Glare1	0.25	0.25	0.57	0.25	0.25	0.22
Glare2	0.26	0.27	0.25	0.30	0.75	0.26
Glare3	0.86	0.25	0.23	0.82	0.25	0.22

Based on the multiobjective optimisation results, the optimal mode of the proposed façade design demonstrates significant improvements. It enhances the appropriate UDI by 69% when compared to the conventional mode. Furthermore, it effectively reduces glare

by 33%, 43% and 59% on occupants located in positions 1, 2 and 3, respectively. Moreover, it generally improves ACH by 38% year-round. Table 6 summarises the ACH, velocity and temperature in the conventional mode of the test cell during critical hours throughout the year. The annual and point-in-time optimisation results, along with the corresponding variables, are detailed in Table 7.

Table 6. Air change per hour, velocity and temperature in conventional mode.

	June			September		
	4 p.m.	1 p.m.	10 a.m.	4 p.m.	1 p.m.	10 a.m.
Air change per hour	140.91	73.62	44.09	130.70	5.23	74.68
Velocity (m/s)	1.1524	0.6021	0.3605	1.0689	0.0427	0.6107
Temperature (°C)	32.2628	33.5414	33.4289	28.7632	30.5502	26.0091

Table 7. The annual and point-in-time optimisation results. UDI stands for Useful Daylight Illuminance and green signifies imperceptible glare. Red represents intolerable glare.

	Current Condition	Optimal Annual Mode	The Most Optimal Instantaneous States					
			June			September		
			10 a.m.	1 p.m.	4 p.m.	10 a.m.	1 p.m.	4 p.m.
Up-Lim-Opening	-	1	2	1	2	2	-	1
Low-Lim-Opening	-	2	2	1	2	2	-	1
Ver-Orientation	-	2	2	2	3	1	-	1
Opening Area	1	1	3	2	2	3	-	2
Air Change per Hour	Table 6	122.27	82.83	122.27	46.49	122.27	-	68.01
UDI(less)%	0.00	0.92	0.89	0.88	0.92	0.82	-	0.87
UDI(App)%	27.97	91.63	90.53	81.97	91.35	85.05	-	82.13
UDI(More)%	71.97	7.63	8.74	17.27	7.93	14.29	-	17.23
Glare1	Table 5	0.20	0.20	0.20	0.19	0.21	-	0.19
Glare2		0.20	0.21	0.21	0.20	0.23	-	0.78
Glare3		0.18	0.18	0.22	0.19	0.21	-	0.19
Average Temperature	Table 6	27.21	31.63	32.74	33.05	27.57	-	25.57
Velocity		0.10	0.12	0.12	0.12	0.14	-	0.12

The optimised façade significantly enhances daylight conditions and airflow management throughout the year, with the most noticeable impact occurring at 10 a.m. in June. However, the façade does not meet comfort criteria, but this issue only arises at 1 p.m. in September. This is primarily because the air velocity falls outside the range required to maintain the desired air changes per hour (ACH). Nonetheless, the façade does not quite meet comfort criteria, with this concern arising at 1 p.m. in September. The main reason is that the air velocity falls outside the range needed to maintain the desired air changes per hour (ACH). During this time, the façade was focused exclusively on conditioning the task surface in terms of visual comfort.

The proposed façade significantly enhances annual daylight performance, particularly in June, especially during the afternoon. It also effectively improves ACH within the comfort range for occupants during the same month, particularly during midday hours. This is due to the potential for direct natural ventilation from outdoor conditions that fall within the comfort zone of interior occupants.

The optimisation results indicate that when using the annual mode (the best possible fixed façade solution) for optimal façade geometry, the best window opening height remained consistent with the current condition, which is 1.2 m. However, in specific months, this height did not yield a single consistent result. It was 0.8 m for mornings and 1.6 m

for the afternoons, illustrating the dynamic nature of window openings and their effectiveness in regulating natural ventilation compared to a fixed, unchanging condition. The algorithm successfully determined the appropriate window opening extent for ensuring human comfort and achieving optimal ACH.

Moreover, the vertical movement of façade modules proved effective in achieving the optimisation goal in this study, with the exception of September. A lower inclination of the sun in the sky, especially in the afternoon, is well managed through the lateral shaping resulting from horizontal movement. This approach is particularly helpful in preventing afternoon glare and, at certain points, allowing more daylight to enter during the later hours of daylight availability from the sides of the windows. However, these vertical façade module movements can partially increase internal air velocity, thereby improving ACH, particularly in the morning. In September, the airflow from outside did not align with the conditions defined in the optimisation process, as the wind was swift and the outside conditions were almost cold. Removing this variable (façade module horizontal movement) could result in an increase in harsh solar radiation, leading to higher overlit and underlit UDI values, especially in the afternoon. This shows that the variable was promising for the success of the façade configuration in achieving human comfort.

Concerning the opening area of the façade modules, the lower and upper limits were defined as variables by the authors. This variable was affected by the position of the sun in the sky in an attraction point. The annual optimum result showed that the 100% upper (completely open) limit and 25% (open as much as 25% of the façade module opening area) lower limit of the opening area of the façade modules were the best option for a fixed façade shape in a year. In simpler terms, when responding to the sun's position in the sky, it was more beneficial for the shading openings to have a pronounced contrast between being fully open and partially closed. A sharp difference in the way they react to sunlight was more advantageous than a uniform distribution of shading openness across the façade. From a fragmented time assessment point of view, the 50% opening area to the upper limit was beneficial for September to improve appropriate UDI, especially in the morning. In addition, this range of open area helped to decrease overlit UDI, while it increased air velocity for enhanced ACH. The 100% range of open area for the façade modules proved inappropriate for the objectives of this study, especially in the afternoon. Additionally, the 50% opening area was beneficial for morning ACH. However, it was harmful in terms of creating glare for positions 2 and 3 (Figure 6). While the 25% opening area was beneficial for improving appropriate UDI in June in the mornings and at noon, it proved to be inappropriate as it increased glare risk for the afternoon in position 1 (Figure 6). This dynamic response to the point-in-time fluctuation of weather conditions proved the superior nature of an adaptive façade compared to fixed ones for human comfort objectives.

To assess the capabilities of Butterfly, the CFD simulation tool and its results were validated. A two-dimensional benchmark test cell (Figure 15) was employed to validate Butterfly's simulation performance and results. This two-dimensional benchmark test, known as the "IEA 2D test case", was established in 1990 for use in IEA Annex 20 research.

The current study utilised this benchmark test to evaluate the CFD performance of room air distribution in Esurance. To achieve this, a box-like room with a supply slot along the side wall was defined within the benchmark. Although the original benchmark was designed for two-dimensional flow testing, subsequent research also investigated results for three-dimensional flow [87]. Figure 13 illustrates the dimensions of the geometry and Table 8 provides a summary of the numerical boundary conditions. Figure 14 displays the bench march model in Rhino3D environment.

The supply inlet was placed near the ceiling on the wall and the supply velocity was set to $U_{in} = 0.455$ m/s. The graph below compares the experimental results with the simulation results in a vertical position ($x = H$ or $x = 3$), in the centre of the z -direction ($z = 0.5H$) and in the rectangular room model.

Figure 16 displays the comparison between the results obtained through practical experiments and those generated by computational fluid dynamics simulations.

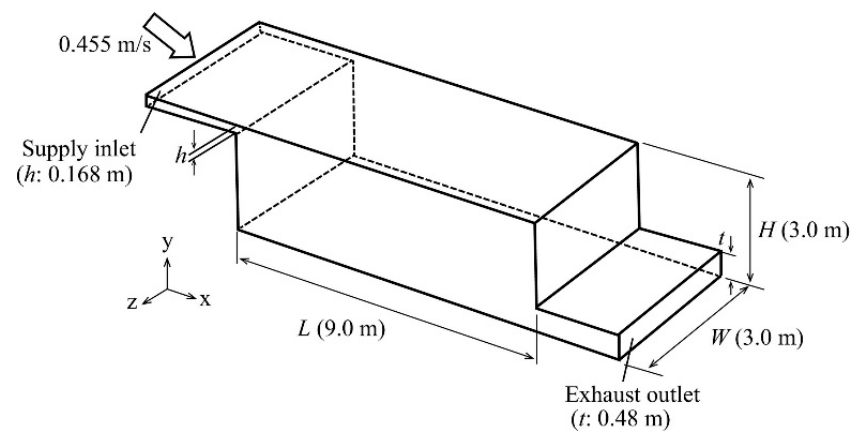


Figure 13. Analysis area of the model of the rectangular room (3D case, Annex benchmark test case); h stands for supply inlet, t stands for exhaust outlet [89].

Table 8. The boundary conditions of the model validation using the IEA Annex 20 benchmark test case [2]; m stands for metre.

Geometry	Height = Width = 3.0 m, Length = 9.0 m, Supply Inlet Height = 0.168 m, Exhaust Outlet Height = 0.48 m
Inflow condition of experiment	$U_{in} = 0.455 \text{ m/s}$ and $TI = 4\%$
Meshes	Structured grid with total of 59,850 meshes
Turbulence model	Standard k-ε model
Inflow boundary	$U_{in} = 0.455 \text{ [m/s]},$
Outflow boundary	$\nabla U_{out} = \nabla k_{out} = \nabla \epsilon_{out} = 0$
Wall treatment:	(Velocity) generalised log law, (Scalar) $\frac{\delta \Phi}{\delta X_i} = 0,$ wall boundary

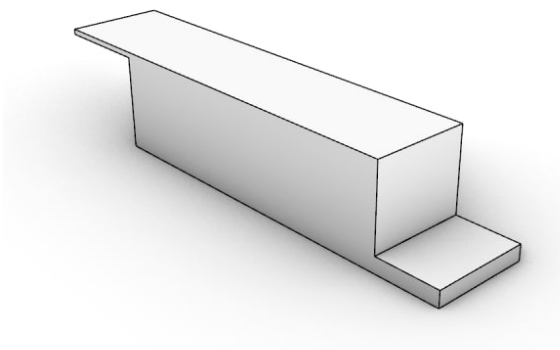


Figure 14. The bench march model (Figure 13) in Rhino3D environment.

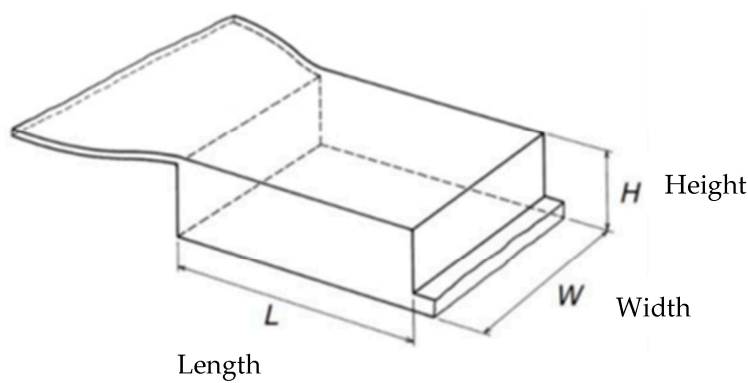


Figure 15. The two-dimensional benchmark test cell geometry [88].

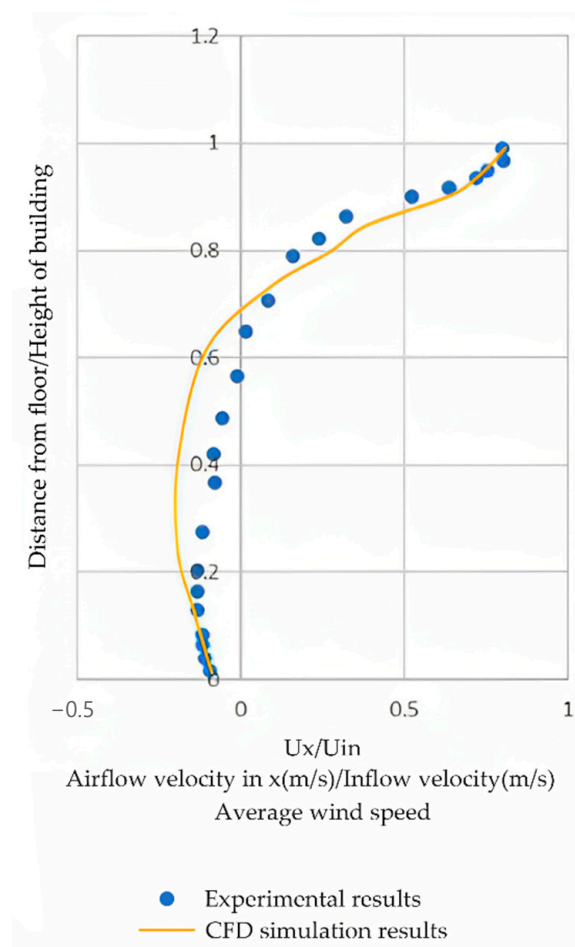


Figure 16. The experimental versus computational fluid dynamic simulation results.

The numerical results agreed with the experimental results. This indicates the high accuracy of the Butterfly plugin, Grasshopper, for CFD simulation.

Figure 17 provides a visual representation of the simulation results, displaying the associations with all alternative variables and outcomes, while also showcasing the best possible result achieved during the optimisation process.

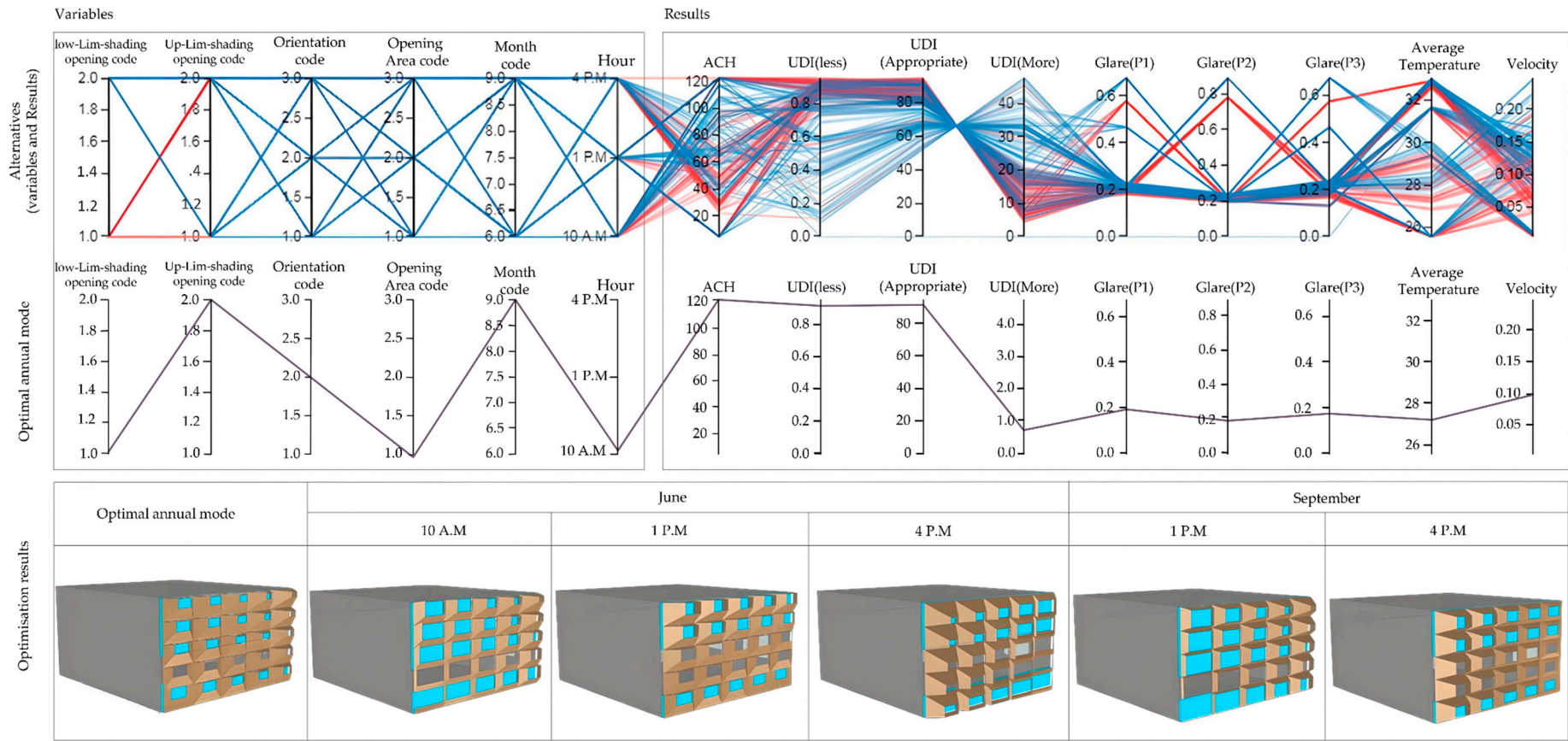


Figure 17. Optimisation workflow (variables and results), annual and critical times of the year optimised solution for enhancing the performance of adaptive façades in daylight and airflow management for human comfort.

5. Discussion

The aim to enhance comfort and energy efficiency was pursued through the utilisation of parametric analysis of daylight and airflow, coupled with the application of computational fluid dynamics (CFD) and multiobjective optimisation. A methodology for building envelope design was provided to designers, with an emphasis placed on the optimisation of visual comfort and the maintenance of air temperature and velocity within the human comfort range.

5.1. Exploring Overlooked Aspects in Prior Studies and Prospect Possibilities

The integration of airflow, ventilation and daylighting within adaptive façade design, along with the consideration of often-overlooked elements such as occupants' location, activities and interior layouts [17,90,91], was emphasised by this study. Many studies have explored kinetic concepts, strategies, principles and criteria for adaptive building envelope design. However, the overlooked aspect of natural ventilation in such studies, in addition to daylight management, increases the risk of sole reliance on HVAC systems for cooling. This overreliance not only impacts energy efficiency but also raises operational costs and carbon footprints. The results showed that integrating a multiobjective approach into an adaptive façade design, such as airflow control for improving ACH, does not jeopardise the enhancement of visual comfort when compared to the sole evaluation of a single-objective façade configuration. Studies that primarily focused on adaptive façades in similar climate conditions yielded nearly identical promising results when compared to this study [10,13,18,19,92].

Findings from the annual optimisation analysis were featured with a focus on the significance of setting the opening area of façade modules to exhibit a distinct contrast between being fully open and partially closed. This approach is contrasted with a more uniform distribution of shading openness, showing a variable influence that has often been overlooked in prior studies that used attraction point-based adaptive façade design [19,93]. This variable's impact can be subject to further investigation and comparison with case studies in diverse climates, each characterised by distinct daylight and outdoor conditions. Such an analysis aims to uncover the full potential and significance of incorporating this variable into studies related to façade design. Figure 18 illustrates examples of façade module opening area distribution.



Figure 18. Examples of façade module opening area distribution; (a): sharp contrast between module area distribution; (b): less contrast between module area distribution.

Moreover, omitting the “façade module horizontal movement” variable increased harsh solar radiation, resulting in higher overlit and underlit UDI values, especially in the afternoon. This underscores the variable's importance in enhancing human comfort within the façade configuration. Similar findings were reported in the Fahmy et al. [11] study on kinetic fins for western façades in low solar altitude areas, albeit without airflow analysis. Additionally, vertical movement of façade modules was found to be effective in achieving the optimisation goals in this study, except for the month of September. This is because of the sun's angle, which allows more direct interior daylight penetration through the façade modules in September compared to June when the sun's angles to the Earth are lower.

The methodology was able to discern the time throughout the year when the objectives were best met and outlined the reasons. For example, the optimised façade significantly

improved daylight conditions and airflow management throughout the year, with the most noticeable impact in June at 10 a.m. However, it falls short of meeting comfort criteria due to air velocity exceeding the desired ACH range, primarily a concern at 1 p.m. in September. The same approach was used by Rizi and Eltaweel (2021) [18] to report on visual comfort performances. However, this novel reporting approach integrates airflow analysis into daylight and parametric design for the first time, aiding in the optimal timing and strategies to enhance daylighting, airflow management and overall human comfort in adaptive building design.

5.2. Building Typology and Activity

As expected, the integration of airflow and daylight simulation and optimisation improved the communication of design requirements within the parametric design process [94]. This integration represents a necessary step towards adaptive architecture [95,96].

In addition, the findings align with the increasing demands of the construction industry for sustainability and occupant well-being. Employing a multiobjective optimisation design methodology across various building typologies (e.g., schools and factories), each customised with specific space comfort metrics, machinery spatial considerations and technical requirements, has the potential to improve indoor air quality (IAQ) and reduce energy consumption. Implementing this integration into practical design processes can lead to more occupant-centric and sustainable building solutions in a holistic approach. This is because the set of boundary conditions can involve human spatial adjustment and needs, informing the appropriate times to utilise or deactivate façade adaptive behaviour [90]. The current study has demonstrated this. The presence of mirrors on the wall and the specification of the height at which airflow should be controlled played significant roles in façade morphology configuration. In other contexts, different factors will exert varying influences. For instance, in educational facilities, classroom layout affects natural lighting, reflections, temperature control, airflow and student thermal comfort. These factors have been highlighted in several studies [97–99] but they have not been widely incorporated into design methodologies.

5.3. Challenges and Possible Solutions

The time-consuming nature of CFD analysis made it difficult to integrate physical aspects of human behaviour into design processes. The design process was time-consuming and necessitated quality hardware system requirements. As a result, it is not uncommon for numerous designers to lean towards more straightforward methodologies in their research [39,100] and to overlook the importance of incorporating factors such as space utilisation, specific activities within the space and furniture arrangement into building façade designs to optimise visual comfort and airflow efficiency. All of these factors are intrinsically interconnected with considerations related to human comfort and building energy efficiency [101,102].

One of the possible available solutions to overcome this limitation might be the use of machine learning after sufficient experimental data collection for a predefined database or real-time data collection [103,104]. However, this is not without its own set of challenges in terms of data quality assurance and quantity, algorithm complexity and interpretability of the results [105].

6. Conclusions

This study developed a parametric methodology to address the critical aspects of visual comfort and airflow with the potential to create sustainable and occupant-centric building solutions.

The optimised façade configuration, compared to the conventional one, demonstrated substantial year-round improvements in key performance metrics. Notably, there was a significant increase in ACH over the course of a year. Additionally, hourly analysis revealed the flexibility of variable selections for optimising both daylight and airflow performance to

accommodate diverse positions and locations of occupants within the test cell. Among the variables, the horizontal movement of the façade module and the attraction patterns within the array of façade modules stood out as particularly promising. The study successfully demonstrated that the integration of parametric daylight and CFD analysis, along with multiobjective optimisation, can lead to improved visual comfort and air quality within the built environment, while consistently maintaining air temperature and velocity within the comfortable range for occupants. This was achieved by strategically defining the boundary conditions to determine the optimal circumstances for implementing natural ventilation by redirecting airflow. Moreover, the façade design methodology discerned when the objectives were best met throughout the year and outlined the reasons.

The primary objective of pioneering an innovative approach to adaptive building envelope design has been realised. The study suggests the need for adaptive architecture across various building typologies and activities, promoting more occupant-centric and sustainable building solutions tailored to specific comfort metrics, spatial considerations and technical requirements. Looking ahead, the research will extend its impact by comparing these simulation-based findings with real-time building energy performance data. While the time-consuming nature of CFD analysis remains a challenge, future solutions, such as machine learning, may offer a way to overcome this limitation.

Author Contributions: Conceptualisation, visualisation, methodology and software, R.A.R. and H.S.; validation, H.S. and K.H.C.; data curation, R.A.R., H.S. and K.H.C.; writing—original draft preparation, R.A.R., H.S. and K.H.C.; writing—review and editing, A.E.; supervision, R.P. All authors have read and agreed to the published version of the manuscript.

Funding: This research received no external funding.

Data Availability Statement: Data are contained within the article.

Conflicts of Interest: The authors declare no conflict of interest.

References

1. Konstantoglou, M.; Tsangrassoulis, A. Dynamic operation of daylighting and shading systems: A literature review. *Renew. Sustain. Energy Rev.* **2016**, *60*, 268–283. [\[CrossRef\]](#)
2. Emmitt, S.; Prins, M.; den Otter, A. (Eds.) *Architectural Management: International Research and Practice*; Wiley-Blackwell: Chichester, UK; Ames, IA, USA, 2009; ISBN 978-1-4051-7786-3.
3. Zuk, W.; Clark, R.H. *Kinetic Architecture*; Van Nostrand Reinhold: New York, NY, USA, 1970; ISBN 978-0-442-15672-5.
4. Schumacher, P. Parametricism: A New Global Style for Architecture and Urban Design. *Archit. Des.* **2009**, *79*, 14–23. [\[CrossRef\]](#)
5. Oxman, R. Performance-Based Design: Current Practices and Research Issues. *Int. J. Archit. Comput.* **2008**, *6*, 1–17. [\[CrossRef\]](#)
6. Zuidgeest, J.; van der Burgh, S.; Kalmeyer, B. Planning by Parameters. *Archit. Des.* **2013**, *83*, 92–95. [\[CrossRef\]](#)
7. Turrin, M.; von Buelow, P.; Stouffs, R. Design explorations of performance driven geometry in architectural design using parametric modeling and genetic algorithms. *Adv. Eng. Inform.* **2011**, *25*, 656–675. [\[CrossRef\]](#)
8. Valentina Sumini, N.B. Performative Building Skin Systems: A Morphogenomic Approach towards Developing Real-Time Adaptive Building Skin Systems. *Int. J. Archit. Comput.* **2009**, *7*, 643–675.
9. Eltaweel, A.; Su, Y. Parametric design and daylighting: A literature review. *Renew. Sustain. Energy Rev.* **2017**, *73*, 1086–1103. [\[CrossRef\]](#)
10. Eltaweel, A.; Su, Y. Controlling venetian blinds based on parametric design; via implementing Grasshopper’s plugins: A case study of an office building in Cairo. *Energy Build.* **2017**, *139*, 31–43. [\[CrossRef\]](#)
11. Fahmy, M.K.; Eltaweel, A.; Rizi, R.A.; Imani, N. Integrated Kinetic Fins for Western Facades in Territories with Low Solar Altitudes. *Buildings* **2023**, *13*, 782. [\[CrossRef\]](#)
12. Tabadkani, A.; Haddadi, M.; Rizi, R.A.; Tabadkani, E. A hierarchical multi-purpose roller shade controller to enhance indoor comfort and energy efficiency. *Build. Simul.* **2023**, *16*, 1239–1256. [\[CrossRef\]](#)
13. Tabadkani, A.; Valinejad Shoubi, M.; Soflaei, F.; Banihashemi, S. Integrated parametric design of adaptive facades for user’s visual comfort. *Autom. Constr.* **2019**, *106*, 102857. [\[CrossRef\]](#)
14. Mahmoud, A.H.A.; Elghazi, Y. Parametric-based designs for kinetic facades to optimize daylight performance: Comparing rotation and translation kinetic motion for hexagonal facade patterns. *Sol. Energy* **2016**, *126*, 111–127. [\[CrossRef\]](#)
15. Al-Masrani, S.M.; Al-Obaidi, K.M. Dynamic shading systems: A review of design parameters, platforms and evaluation strategies. *Autom. Constr.* **2019**, *102*, 195–216. [\[CrossRef\]](#)
16. Soflaei, F.; Shokouhian, M.; Zhu, W. Socio-environmental sustainability in traditional courtyard houses of Iran and China. *Renew. Sustain. Energy Rev.* **2017**, *69*, 1147–1169. [\[CrossRef\]](#)

17. Rizi, R.A. Occupants' migration in residential buildings towards comfort and energy efficiency (case of traditional residential architecture in Iran). *J. Hous. Built Environ.* **2022**, *37*, 179–211. [\[CrossRef\]](#)
18. Rizi, R.A.; Eltaweel, A. A user detective adaptive facade towards improving visual and thermal comfort. *J. Build. Eng.* **2020**, *33*, 101554. [\[CrossRef\]](#)
19. Hosseini, S.M.; Mohammadi, M.; Guerra-Santin, O. Interactive kinetic façade: Improving visual comfort based on dynamic daylight and occupant's positions by 2D and 3D shape changes. *Build. Environ.* **2019**, *165*, 106396. [\[CrossRef\]](#)
20. Widén, J.; Wäckelgård, E. A high-resolution stochastic model of domestic activity patterns and electricity demand. *Appl. Energy* **2010**, *87*, 1880–1892. [\[CrossRef\]](#)
21. Prieto, A.; Knaack, U.; Auer, T.; Klein, T. Passive cooling & climate responsive façade design. *Energy Build.* **2018**, *175*, 30–47. [\[CrossRef\]](#)
22. Aflaki, A.; Hirbodi, K.; Mahyuddin, N.; Yaghoubi, M.; Esfandiari, M. Improving the air change rate in high-rise buildings through a transom ventilation panel: A case study. *Build. Environ.* **2019**, *147*, 35–49. [\[CrossRef\]](#)
23. Roetzel, A.; Tsangrassoulis, A.; Dietrich, U.; Busching, S. A review of occupant control on natural ventilation. *Renew. Sustain. Energy Rev.* **2010**, *14*, 1001–1013. [\[CrossRef\]](#)
24. Meyers, R.A. (Ed.) *Encyclopedia of Sustainability Science and Technology*; Springer New York: New York, NY, USA, 2012; ISBN 978-0-387-89469-0.
25. Solgi, E.; Hamedani, Z.; Fernando, R.; Skates, H.; Orji, N.E. A literature review of night ventilation strategies in buildings. *Energy Build.* **2018**, *173*, 337–352. [\[CrossRef\]](#)
26. Yoon, N.; Malkawi, A. *Predicting the Effectiveness of Wind-Driven Natural Ventilation Strategy for Interactive Building Design*; International Building Performance Simulation Association: Rapid City, SD, USA, 2017.
27. Karagkouni, C.; Fatah gen Schieck, A.; Tsigkari, M.; Chroni, A. Façade Apertures Optimization: Integrating Cross-Ventilation Performance Analysis in Fluid Dynamics Simulation. In Proceedings of the 2013 Spring Simulation Multiconference, San Diego, CA, USA, 7–10 April 2013.
28. Arinami, Y.; Akabayashi, S.; Tominaga, Y.; Sakaguchi, J. Performance evaluation of single-sided natural ventilation for generic building using large-eddy simulations: Effect of guide vanes and adjacent obstacles. *Build. Environ.* **2019**, *154*, 68–80. [\[CrossRef\]](#)
29. Assimakopoulos, M.N.; Tsangrassoulis, A.; Mihalakakou, G.; Santamouris, M.; Jauré, S. Development of a control algorithm to optimize airflow rates through variable size windows. *Energy Build.* **2002**, *34*, 363–368. [\[CrossRef\]](#)
30. Sacht, H.; Lukiantchuki, M.A. Windows Size and the Performance of Natural Ventilation. *Procedia Eng.* **2017**, *196*, 972–979. [\[CrossRef\]](#)
31. Cimmino, M.C.; Miranda, R.; Sicignano, E.; Ferreira, A.J.M.; Skelton, R.E.; Fraternali, F. Composite solar façades and wind generators with tensegrity architecture. *Compos. Part B Eng.* **2017**, *115*, 275–281. [\[CrossRef\]](#)
32. Shafaghat, A.; Keyvanfar, A. Dynamic façades design typologies, technologies, measurement techniques, and physical performances across thermal, optical, ventilation, and electricity generation outlooks. *Renew. Sustain. Energy Rev.* **2022**, *167*, 112647. [\[CrossRef\]](#)
33. Andreeva, D.; Nemova, D.; Kotov, E. Multi-Skin Adaptive Ventilated Facade: A Review. *Energies* **2022**, *15*, 3447. [\[CrossRef\]](#)
34. Alkhatib, H.; Lemarchand, P.; Norton, B.; O'Sullivan, D.T.J. Deployment and control of adaptive building facades for energy generation, thermal insulation, ventilation and daylighting: A review. *Appl. Therm. Eng.* **2021**, *185*, 116331. [\[CrossRef\]](#)
35. Napier, J. Climate Based Façade Design for Business Buildings with Examples from Central London. *Buildings* **2015**, *5*, 16–38. [\[CrossRef\]](#)
36. Johnsen, K.; Winther, F.V. Dynamic Facades, the Smart Way of Meeting the Energy Requirements. *Energy Procedia* **2015**, *78*, 1568–1573. [\[CrossRef\]](#)
37. Attia, S. Evaluation of adaptive facades: The case study of Al Bahr Towers in the UAE. *QScience Connect* **2017**, *2017*, 6. [\[CrossRef\]](#)
38. Sun, N.; Cui, Y.; Jiang, Y.; Li, S. Lighting and Ventilation-based Building Sun-Shading Design and Simulation Case in Cold Regions. *Energy Procedia* **2018**, *152*, 462–469. [\[CrossRef\]](#)
39. Omar Elshiwihy, S.; Nasarullah Chaudhry, H. Parametric Study on Determining Optimum Shading Techniques for Urban High-Rise Dwellings. *Urban Sci.* **2019**, *3*, 85. [\[CrossRef\]](#)
40. Barozzi, G.S.; Grossa, R. Shading effect of eggcrate devices on vertical windows of arbitrary orientation. *Sol. Energy* **1987**, *39*, 329–341. [\[CrossRef\]](#)
41. Hosseini, S.M.; Mohammadi, M.; Rosemann, A.; Schröder, T.; Lichtenberg, J. A morphological approach for kinetic façade design process to improve visual and thermal comfort: Review. *Build. Environ.* **2019**, *153*, 186–204. [\[CrossRef\]](#)
42. Rutten, D. Galapagos: On the Logic and Limitations of Generic Solvers. *Archit. Des.* **2013**, *83*, 132–135. [\[CrossRef\]](#)
43. McNeel & Associates Grasshopper—New in Rhino 6. Available online: <https://www.rhino3d.com/6/new/grasshopper/> (accessed on 26 September 2023).
44. Carlucci, S.; Causone, F.; De Rosa, F.; Pagliano, L. A review of indices for assessing visual comfort with a view to their use in optimization processes to support building integrated design. *Renew. Sustain. Energy Rev.* **2015**, *47*, 1016–1033. [\[CrossRef\]](#)
45. Jahangiri, M.; Rizi, R.A.; Shamsabadi, A.A. Feasibility study on simultaneous generation of electricity and heat using renewable energies in Zarrin Shahr, Iran. *Sustain. Cities Soc.* **2018**, *38*, 647–661. [\[CrossRef\]](#)
46. Epwmap. Available online: <http://www.ladybug.tools/epwmap/> (accessed on 2 February 2019).

47. Tsigonia, A.; Lagoudi, A.; Chandrinou, S.; Linos, A.; Evlogias, N.; Alexopoulos, E.C. Indoor Air in Beauty Salons and Occupational Health Exposure of Cosmetologists to Chemical Substances. *Int. J. Environ. Res. Public Health* **2010**, *7*, 314–324. [CrossRef]
48. Minerva Beauty. Three Salon Floor Plans, One 800 Square-Foot Space. Available online: <https://www.minervabeauty.com> (accessed on 26 September 2023).
49. Baaghideh, M.; Mayvaneh, F.; Shekari badi, A.; Shojaei, T. Evaluation of human thermal comfort using UTCI index: Case study Khorasan Razavi, Iran. *Nat. Environ. Chang.* **2016**, *2*, 165–175.
50. ANSI/ASHRAE Standard 55-2017; ANSI/ASHRAE Standard 55, Thermal Environmental Conditions for Human Occupancy, Aamerican Standard. ANSI: New York, NY, USA, 2017.
51. Guo, B. *Infinite-Dimensional Dynamical Systems; Attractors and Methods*; De Gruyter: Berlin, Germany; Boston, MA, USA, 2018; Volume 2, ISBN 978-3-11-058726-5.
52. Health (Hairdressers) Regulations 1980 (SR 1980/143) (as at 01 July 2014)—New Zealand Legislation. Available online: <https://www.legislation.govt.nz/regulation/public/1980/0143/latest/whole.html> (accessed on 30 September 2023).
53. Luo, J.-F.; Yang, Z.-Y.; Yi, H.-Q.; Yang, Z.-D. Study on the Reflection Characteristics of Ceramic Tile Building Materials to Solar Radiation. In *ESSE 2017*; Wang, Y., Ed.; De Gruyter: Berlin, Germany, 2017; pp. 153–170. ISBN 978-3-11-054004-8.
54. Abdollahi Rizi, R.; Bagherzadeh, F.; Schnabel, M.A.; Bakshi, N. A design methodology to consider occupants' spatial adjustment and manage view content in adaptive façade design for improving visual comfort. *Archit. Eng. Des. Manag.* **2023**, *1*–23. [CrossRef]
55. Lister, T.; Wright, P.A.; Chappell, P.H. Optical properties of human skin. *J. Biomed. Opt.* **2012**, *17*, 0909011. [CrossRef] [PubMed]
56. Ladybug Tools | Honeybee. Available online: <https://www.ladybug.tools/honeybee.html> (accessed on 18 June 2020).
57. Nabil, A.; Mardaljevic, J. Useful daylight illuminances: A replacement for daylight factors. *Energy Build.* **2006**, *38*, 905–913. [CrossRef]
58. Nabil, A.; Mardaljevic, J. Useful daylight illuminance: A new paradigm for assessing daylight in buildings. *Light. Res. Technol.* **2005**, *37*, 41–57. [CrossRef]
59. U.S. Green Building Council. *Leadership in Energy and Environmental Design (LEED)*; LEED v4 for Building Design and Construction; U.S. Green Building Council: Washington, DC, USA, 2015.
60. Wienold, J.; Christoffersen, J. Towards a new daylight glare rating. In *Licht für den Menschen*; Ludwig Erhard Haus Industrie-und Handelskammer zu Berlin: Berlin, Germany, 2005.
61. Wienold, J.; Christoffersen, J. Evaluation methods and development of a new glare prediction model for daylight environments with the use of CCD cameras. *Energy Build.* **2006**, *38*, 743–757. [CrossRef]
62. Jones, N.L.; Reinhart, C.F. Experimental validation of ray tracing as a means of image-based visual discomfort prediction. *Build. Environ.* **2017**, *113*, 131–150. [CrossRef]
63. Etheridge, D. *Natural Ventilation of Buildings: Theory, Measurement and Design*; Wiley: Hoboken, NJ, USA, 2012; ISBN 978-1-119-95178-0.
64. Jiang, Y.; Allocca, C.; Chen, Q. Validation of CFD Simulations for Natural Ventilation. *Int. J. Vent.* **2004**, *2*, 359–369. [CrossRef]
65. Ladybug Tools | Butterfly. Available online: <https://www.ladybug.tools/butterfly.html> (accessed on 18 June 2020).
66. Elwy, I.; Ibrahim, Y.; Fahmy, M.; Mahdy, M. Outdoor microclimatic validation for hybrid simulation workflow in hot arid climates against ENVI-met and field measurements. *Energy Procedia* **2018**, *153*, 29–34. [CrossRef]
67. Engys Ltd. *A Comprehensive Tour of Snappyhexmesh (7th Openfoam Workshop)*; Engys Ltd.: London, UK, 2012.
68. Hex-Dominant Meshing | SimScale CAE Documentation. Available online: <https://www.simscale.com/docs/simulation-setup/meshing/hex-dominant/> (accessed on 3 November 2020).
69. Zhao, Y.; Li, R.; Feng, L.; Wu, Y.; Niu, J.; Gao, N. Boundary layer wind tunnel tests of outdoor airflow field around urban buildings: A review of methods and status. *Renew. Sustain. Energy Rev.* **2022**, *167*, 112717. [CrossRef]
70. Bre, F.; Gimenez, J.M. A cloud-based platform to predict wind pressure coefficients on buildings. *Build. Simul.* **2022**, *15*, 1507–1525. [CrossRef] [PubMed]
71. Hu, Y.; Xu, F.; Gao, Z. A Comparative Study of the Simulation Accuracy and Efficiency for the Urban Wind Environment Based on CFD Plug-Ins Integrated into Architectural Design Platforms. *Buildings* **2022**, *12*, 1487. [CrossRef]
72. Franke, J.; Hirsch, C.; Jensen, A.G.; Krüs, H.W.; Schatzmann, M.; Westbury, P.S.; Miles, S.D.; Wisse, J.A.; Wright, N.G. Recommendations on the Use of Cfd in Wind Engineering. In *Proceedings of the International Conference on Urban Wind Engineering and Building Aerodynamics: Cost Action, Sint-Genesius-Rode, Belgium, 5–7 May 2004*; Volume 14.
73. Allocca, C.; Chen, Q.; Glicksman, L.R. Design analysis of single-sided natural ventilation. *Energy Build.* **2003**, *35*, 785–795. [CrossRef]
74. Del Rio, M.A.; Asawa, T.; Hirayama, Y. Modeling and Validation of the Cool Summer Microclimate Formed by Passive Cooling Elements in a Semi-Outdoor Building Space. *Sustainability* **2020**, *12*, 5360. [CrossRef]
75. Guerrero, J.; Cominetti, A.; Pralits, J.; Villa, D. Surrogate-Based Optimization Using an Open-Source Framework: The Bulbous Bow Shape Optimization Case. *Math. Comput. Appl.* **2018**, *23*, 60. [CrossRef]
76. Stiapis, C.S.; Skouras, E.D.; Burganos, V.N. Three-Dimensional Digital Reconstruction of Ti2AlC Ceramic Foams Produced by the Gelcast Method. *Materials* **2019**, *12*, 4085. [CrossRef]
77. Kaseb, Z.; Hafezi, M.; Tahbaz, M.; Delfani, S. A framework for pedestrian-level wind conditions improvement in urban areas: CFD simulation and optimization. *Build. Environ.* **2020**, *184*, 107191. [CrossRef]
78. Montazeri, H.; Blocken, B.; Derome, D.; Carmeliet, J.; Hensen, J.L.M. CFD analysis of forced convective heat transfer coefficients at windward building facades: Influence of building geometry. *J. Wind Eng. Ind. Aerodyn.* **2015**, *146*, 102–116. [CrossRef]

79. Blocken, B.; Janssen, W.D.; van Hooff, T. CFD simulation for pedestrian wind comfort and wind safety in urban areas: General decision framework and case study for the Eindhoven University campus. *Environ. Model. Softw.* **2012**, *30*, 15–34. [\[CrossRef\]](#)
80. Yuan, C.; Ng, E. Building porosity for better urban ventilation in high-density cities—A computational parametric study. *Build. Environ.* **2012**, *50*, 176–189. [\[CrossRef\]](#)
81. Blocken, B. Computational Fluid Dynamics for urban physics: Importance, scales, possibilities, limitations and ten tips and tricks towards accurate and reliable simulations. *Build. Environ.* **2015**, *91*, 219–245. [\[CrossRef\]](#)
82. Tan, H.; Wong, K.Y.; Othman, M.H.D.; Kek, H.Y.; Nyakuma, B.B.; Ho, W.S.; Hashim, H.; Wahab, R.A.; Sheng, D.D.C.V.; Wahab, N.H.A.; et al. Why do ventilation strategies matter in controlling infectious airborne particles? A comprehensive numerical analysis in isolation ward. *Build. Environ.* **2023**, *231*, 110048. [\[CrossRef\]](#)
83. Tan, H.; Wong, K.Y.; Othman, M.H.D.; Nyakuma, B.B.; Vui Sheng, D.D.C.; Kek, H.Y.; Ho, W.S.; Hashim, H.; Chiong, M.C.; Zubir, M.A.; et al. Does human movement-induced airflow elevate infection risk in burn patient's isolation ward? A validated dynamics numerical simulation approach. *Energy Build.* **2023**, *283*, 112810. [\[CrossRef\]](#)
84. ASHRAE ASHRAE 62.1-2010; Ventilation for Acceptable Indoor Air Quality. ASHRAE: Atlanta, GA, USA, 2004.
85. Chronis, A.; Dubor, A.; Cabay, E. Mostapha Sadeghipour Roudsari Integration of CFD in Computational Design—An evaluation of the current state of the art. *Int. J. Archit. Comput.* **2019**, *1*, 601–610. [\[CrossRef\]](#)
86. Lechner, N. *Heating, Cooling, Lighting: Sustainable Design Methods for Architects*, 4th ed.; John Wiley & Sons, Inc.: Hoboken, NJ, USA, 2015; ISBN 978-1-118-58242-8.
87. Nielsen, P.V.; Rong, L.; Cortes, I.O. The IEA annex 20 two-dimensional benchmark test for CFD predictions. In Proceedings of the Clima 2010: 10th IEA World Congress: Sustainable Energy Use in Buildings, Antalya, Turkey, 9–12 May 2010.
88. Nielsen, P.V. *Specification of a Two-Dimensional Test Case: (IEA)*; Gul Serie; Institut for Bygningsteknik, Aalborg Universitet: Aalborg, Denmark, 1990; Volume R9040.
89. Lim, E.; Sandberg, M.; Ito, K. Returning characteristics of pollutants for a local domain in the presence of returning and recirculating airflow in indoor environments. *Indoor Air* **2021**, *31*, 1267–1280. [\[CrossRef\]](#) [\[PubMed\]](#)
90. Wagner, A.; O'Brien, W.; Dong, B. (Eds.) *Exploring Occupant Behavior in Buildings*; Springer International Publishing: Cham, Switzerland, 2018; ISBN 978-3-319-61463-2.
91. Memarian, G.; Sadoughi, A. Application of access graphs and home culture: Examining factors relative to climate and privacy in Iranian houses. *Sci. Res. Essays* **2011**, *6*, 6350–6363. [\[CrossRef\]](#)
92. Koo, S.Y.; Yeo, M.S.; Kim, K.W. Automated blind control to maximize the benefits of daylight in buildings. *Build. Environ.* **2010**, *45*, 1508–1520. [\[CrossRef\]](#)
93. Goharian, A.; Daneshjoo, K.; Mahdavinjad, M.; Yeganeh, M. Voronoi geometry for building facade to manage direct sunbeams. *J. Sustain. Archit. Civ. Eng.* **2022**, *31*, 109–124. [\[CrossRef\]](#)
94. Maksoud, A.; Hussien, A.; Mushtaha, E.; Alawneh, S.I.A.-R. Computational Design and Virtual Reality Tools as an Effective Approach for Designing Optimization, Enhancement, and Validation of Islamic Parametric Elevation. *Buildings* **2023**, *13*, 1204. [\[CrossRef\]](#)
95. Sassi, P. *Strategies for Sustainable Architecture*; Taylor & Francis: Abingdon, UK, 2006; ISBN 978-0-415-34142-4.
96. Gosling, J.; Sassi, P.; Naim, M.; Lark, R. Adaptable buildings: A systems approach. *Sustain. Cities Soc.* **2013**, *7*, 44–51. [\[CrossRef\]](#)
97. Daisey, J.M.; Angell, W.J.; Apte, M.G. Indoor air quality, ventilation and health symptoms in schools: An analysis of existing information: Indoor air quality, ventilation and health symptoms in schools. *Indoor Air* **2003**, *13*, 53–64. [\[CrossRef\]](#) [\[PubMed\]](#)
98. Lourenço, P.; Pinheiro, M.D.; Heitor, T. Light use patterns in Portuguese school buildings: User comfort perception, behaviour and impacts on energy consumption. *J. Clean. Prod.* **2019**, *228*, 990–1010. [\[CrossRef\]](#)
99. Catalina, T.; Iordache, V. IEQ assessment on schools in the design stage. *Build. Environ.* **2012**, *49*, 129–140. [\[CrossRef\]](#)
100. Shen, C.; Li, X. Thermal performance of double skin façade with built-in pipes utilizing evaporative cooling water in cooling season. *Sol. Energy* **2016**, *137*, 55–65. [\[CrossRef\]](#)
101. Kwon, M.; Remøy, H.; van den Bogaard, M. Influential design factors on occupant satisfaction with indoor environment in workplaces. *Build. Environ.* **2019**, *157*, 356–365. [\[CrossRef\]](#)
102. Al-Mumin, A.; Khattab, O.; Sridhar, G. Occupants' behavior and activity patterns influencing the energy consumption in the Kuwaiti residences. *Energy Build.* **2003**, *35*, 549–559. [\[CrossRef\]](#)
103. Shafighfard, T.; Bagherzadeh, F.; Rizi, R.A.; Yoo, D.-Y. Data-driven compressive strength prediction of steel fiber reinforced concrete (SFRC) subjected to elevated temperatures using stacked machine learning algorithms. *J. Mater. Res. Technol.* **2022**, *21*, 3777–3794. [\[CrossRef\]](#)
104. Vinuesa, R.; Brunton, S.L. Enhancing computational fluid dynamics with machine learning. *Nat. Comput. Sci.* **2022**, *2*, 358–366. [\[CrossRef\]](#)
105. Carbone, M.R. When not to use machine learning: A perspective on potential and limitations. *MRS Bull.* **2022**, *47*, 968–974. [\[CrossRef\]](#)

Disclaimer/Publisher's Note: The statements, opinions and data contained in all publications are solely those of the individual author(s) and contributor(s) and not of MDPI and/or the editor(s). MDPI and/or the editor(s) disclaim responsibility for any injury to people or property resulting from any ideas, methods, instructions or products referred to in the content.